Hindawi
Journal of Advanced Transportation
Volume 2020, Article ID 8865814, 23 pages
https://doi.org/10.1155/2020/8865814

Research Article

An Asymmetric-Anticipation Car-following Model in the Era of Autonomous-Connected and Human-Driving Vehicles

Ammar Jafaripournimchahi,[1] **Wusheng Hu**,[1] **and Lu Sun**[2]

[1]*School of Transportation Engineering, Southeast University, Nanjing 210096, China*
[2]*Department of Civil and Environmental Engineering, University of Maryland, College Park, MD, USA*

Correspondence should be addressed to Wusheng Hu; wusheng.hu@163.com

Received 7 July 2020; Revised 8 September 2020; Accepted 28 September 2020; Published 29 October 2020

Academic Editor: Haneen Farah

Herein, we explored the impact of anticipation and asymmetric driving behavior on vehicle's position, velocity, acceleration, energy consumption, and exhaust emissions of CO, HC, and NO_x in mixed traffic flow. We present an asymmetric-anticipation car-following model (AAFVD) considering the motion information from two direct preceding vehicles (i.e., human-driving (HD) and autonomous and connected (AC) vehicles platoon) via wireless data transmission. The linear stability approach was used to evaluate the properties of the AAFVD model. Our simulations revealed that the drivers' anticipation factor using the motion information from two direct preceding vehicles in connected vehicles environment can effectively improve traffic flow stability. The vehicle's departure and arrival process while passing through a signal lane with a traffic light considering the anticipation and asymmetric driving behavior, and the motion information from two direct preceding vehicles was explored. Our numerical results demonstrated that the AAFVD model can decrease the velocity fluctuations, energy consumption, and exhaust emissions of vehicles in mixed traffic flow system.

1. Introduction

Many existing human-driving car-following models have introduced to capture the process of the drivers' behavior individually, traveling in various contexts on the road without any overtaking.

Since the 1990s, they have become more important due to using in design and evaluating different ITS (intelligent transportation system) control strategies and technologies. The last decade has witnessed a rapid development of communication and information technologies. The wireless communication systems have been advanced significantly, which enables vehicle-to-vehicle (V2V) communication and creates a vast opportunity to improve the vehicle's operation on the road [1–5].

With the goal of increasing the drivers' comfort and safety and reducing energy consumption and the exhaustion of greenhouse emissions, many famous manufacturers like BMW, Audi, and Ford aim to start testing automated vehicles by 2020 [6, 7].

The penetration rate of autonomous and connected (AC) vehicles is currently low.

It is expected to increase gradually in the global market for upcoming years. Thus, there would be a long transition time from human-driving (HD)vehicles to autonomous and connected (AC) vehicles [8–12].

During the transition time, there would be a mixed traffic flow of human-driving and autonomous vehicles on the roads. Several researchers acknowledged that the behavior of traffic flow significantly will change, when the number of autonomous vehicles increases.

Thus, it is essential to study the effect of autonomous and human-driving (mixed traffic flow) behavior on traffic flow to reduce the costly mistakes before the widespread implementation.

Over the past decades, most of the studies focused on the dynamic evolutions of human-driving traffic flow, barely considering the dynamic evolutions of human-driving vehicles equipped with V2V communication technology in mixed traffic flow [13–18].

Human-driving car-following models can be categorized into four groups: General Motors (GM) models, desired measures models, safety distances or collision avoidance models, and optimal velocity models. The main features of these models are summarized in Table 1.

The first version of linear car-following models was proposed by Chandler et al. [19] and Herman et al. [20] based on stimulus-response. Gazis et al. [21] proposed the first version of nonlinear models by including more general sensitivity terms. Although the model has the merit of being simple, it does so with some limitations. These limitations include impractical acceleration for very low traffic densities ($S \longrightarrow \infty$), overestimation of the human ability to perceive small alterations in various circumstances, and ignoring the physical limitations of the acceleration process.

The acceleration/deceleration and the relative velocity are linearly linked to each other in contrast to actual experiments [29]; when the preceding vehicle's velocity is very high compared to the following vehicle's velocity, the relative velocity approaches infinity ($\Delta v \longrightarrow \infty$).

Treiber et al. [22] proposed an intelligent driver model (IDM) by considering both the desired velocity and the desired space headway. Most parameters in desired models are unobservable in nature, so this makes their estimation more challenging. Therefore, many of the desired models are not estimated using real traffic data.

A nonlinear version of safety distances models was proposed by Newell [23] to solve the deficiency of existing car-following models in extremely low densities, by presuming that the following vehicle's velocity has a nonlinear relationship with the vehicular gap.

However, Newell's model fixed the deficiency of existing car-following models in extremely low densities; there are still some problems. This model supposed that a driver adopts his/her vehicle's velocity by taking the vehicular gap into account with the delay time τ.

Bando et al. [24] proposed a remarkable car-following model called the OVM based on the assumption that the optimal velocity of the following vehicle was determined by his/her own vehicular gap to modify the shortcoming in Newell's model. The OVM has a good ability to reveal many complex dynamic phenomena of vehicular traffic such as nonequilibrium vehicular flow, jam information, and stop-and-go waves. But the OVM could not resolve the problem of unrealistic acceleration and deceleration because the OV function only depends on the vehicular gap and density which affects the model heavily.

To overcome the dilemma of impractical deceleration in OVM, Helbing and Tilch [25] extended the OVM by incorporating the relative velocity and created the generalized force (GF) model.

Jiang et al. [26] presented the full velocity difference (FVD) model by taking negative and positive relative velocity into consideration to overcome incapability of the GM model in the delay time and the velocity of the kinematic wave at traffic jam.

According to the simulations, the deceleration and acceleration of the FVD model do not fall into the empirical region $[-3\ \mathrm{m/s^2}, 4\ \mathrm{m/s^2}]$ proposed by Helbing and Tilch [25], and the deceleration of the FVD model is extremely high.

Ge et al. [27] have taken the relative velocities of two direct preceding vehicles into account and obtained a novel car-following model (two-velocity difference (TVD) model) to improve the OV model:

$$\frac{\mathrm{d}v_n(t)}{\mathrm{d}t} = a\left[V_o\left(S_n(t)\right) - v_n(t)\right] + \lambda\left(p\Delta v_n(t) + (1-p)\Delta v_{n+1}(t)\right), \tag{1}$$

where p is the weight coefficient and λ is the sensitive constant. Numerical simulations indicate that the two-velocity difference model provides a superior match with the traffic trajectory data than the OVM and the GFM due to the application of the ITS.

Zhao et al. [30] constructed a two-dimensional vehicular movement model based on optimal control to study driving behavior (i.e., turning the steering wheel and pushing the brake or throttle pedals) of HD vehicles at intersections. The results provided a new insight for the future implementation of signal control strategies.

Focusing on the application of the traffic flow model, Zhao et al. [31] developed the FVD model considering the interaction between vehicle yielding and pedestrian gap acceptance (VY and PGA) at midblock crosswalks to explore the impacts of the interaction on traffic flow.

Tang et al. [32] incorporated a speed guidance strategy in the car-following model to investigate the driving behavior and the fuel consumption in a single-lane road with multiple signalized intersections. The findings provided a new insight supporting the eco-driving strategies near the signalized intersections.

Although the aforementioned models used many specific aspects in simulating the dynamics of human-driving traffic flow, they did not consider that the driver's reaction is slower in acceleration than in deceleration in real traffic flow, which is called asymmetric driving behavior.

Based on the asymmetric driving assumption, Gong et al. [28] proposed the AFVD model by taking two different sensitivity parameters into account, as shown in the following equation:

$$\frac{\mathrm{d}v_n(t)}{\mathrm{d}t} = a\left[V_o\left(\Delta x_n(t)\right) - v_n(t)\right] + \lambda_1\left(\Delta v_n(t)\right) \cdot H\left(-\Delta v_n(t)\right) + \lambda_2\left(\Delta v_n(t)\right) \cdot H\left(-\Delta v_n(t)\right), \tag{2}$$

where H is a Heaviside step function. It is presumed that the capability of vehicles in acceleration is lower than that in deceleration.

Shamoto et al. [29] derived an asymmetric car-following model based on the experiments:

$$\frac{\mathrm{d}v_n(t)}{\mathrm{d}t} = a - b\frac{v_n}{\left(h_n - d\right)^2}\exp\left(-c\Delta v_n(t)\right) - \gamma v_n, \tag{3}$$

where a, b, c, d, γ are positive parameters.

With the development of ITS, the driver can acquire information from the preceding vehicles which affects the

Table 1: Car-following models.

Model category	Model name	Distinctive features and advantages	Limitations	Reference
General Motors models	Linear model	Simplest model	Too simple to model all realistic traffic phenomena	[19, 20]
			Impractical acceleration for very low traffic densities ($S \longrightarrow \infty$)	
			Ignoring velocity differences between vehicles	
		The stability of the model is proved	Ignoring the physical limitation of the acceleration process	
			Ignoring anticipation driving behavior	
			Ignoring asymmetric driving behavior	
	Nonlinear model	Simple and well-established model	Use of identical reaction time for all drivers does not capture interdriver heterogeneity	[21]
		Driver reaction time is considered	Human ability is overestimated	
			Ignoring acceleration and deceleration	
			Very sensitive to velocity differences	
		Model parameter can be easily estimated from either vehicle trajectory data or macroscopic data	Ignoring velocity differences between vehicles	
			Ignoring the physical limitation of the acceleration process	
			Ignoring anticipation driving behavior	
			Ignoring asymmetric driving behavior	
Desired measures models	Intelligent driver (ID) model	Considering both desired velocity and desired headway	Ignoring reaction time	[22]
		Considering traffic capacity	Ignoring the physical limitation of the acceleration process	
			Ignoring anticipation driving behavior	
			Ignoring asymmetric driving behavior	
Safety distance models	Newell model	Follows stimulus-response type function	Produces unrealistic deceleration and acceleration	[23]
			Ignoring the physical limitation of the acceleration process	
			Ignoring anticipation driving behavior	
			Ignoring asymmetric driving behavior	

Table 1: Continued.

Model category	Model name	Distinctive features and advantages	Limitations	Reference
Optimal velocity models	Optimal velocity (OV) model	Depends on distance from the preceding car	Produces unrealistic deceleration and acceleration Unrealistically sensitive to reaction time Ignoring the physical limitation of the acceleration process Ignoring anticipation driving behavior Ignoring asymmetric driving behavior Ignoring the velocity differences between vehicles	[24]
	GF model	Resolved unrealistic deceleration and acceleration problem Parameters have been estimated from real data	Driver reaction time is ignored There is still unrealistic deceleration acceleration Ignoring the physical limitation of the acceleration process Ignoring anticipation driving behavior Ignoring asymmetric driving behavior	[25]
	Full velocity differences (FVD) model	Velocity difference is explicitly included to overcome unrealistic deceleration and acceleration depicting many complex phenomena in real traffic, such as shock waves, rarefaction waves, stop-and-go waves, and local cluster effects	Driver reaction time is ignored Parameters have not been estimated from real data Ignoring the physical limitation of the acceleration process Ignoring anticipation driving behaviour Ignoring asymmetric driving behavior	[26]
	Two-velocity difference (TVD) model	Successful in describing the deceleration process, congestion, instability, and stop-and-go traffic	Ignoring the physical limitation of the acceleration process Ignoring anticipation driving behavior Ignoring asymmetric driving behavior	[27]
	Asymmetric (FVD) model	Considered asymmetric driving behavior	Ignoring the physical limitation of the acceleration process Ignoring anticipation driving behavior Ignoring reaction time	[28]
	Asymmetric-anticipation FVD (AAFVD) model	Considered anticipation driving behavior Considered asymmetric driving behavior A model with more generalizability Considered two preceding vehicles motion information	A brand-new model needs more investigation of its characteristic	This paper

driving behavior. In the last few years, several studies have been done to enhance the realism of existing car-following models by taking the vehicular gap of several preceding vehicles, their relative velocities, or both parameters into consideration in the ITS environment [33–39].

These studies described that taking the motion information from several preceding vehicles into consideration can make safe driving more possible.

Furthermore, real driving experience suggests that a driver may be influenced by not only the motion status of multiple preceding vehicles but also the anticipation driving behavior according to his/her perception of downstream traffic flow.

An extended car-following model with the consideration of the estimation of the vehicular gap between the flowing vehicle and the preceding vehicle was put forward by Zheng et al. [40] to explore the impacts of anticipation driving behavior on traffic flow.

The aforementioned models were established to capture the driving behavior of HD vehicles. The deficiency of these models lies in the fact that they are not suitable to study mixed traffic flow including human-driving and AC vehicles

[41–43] due to the limitation of their accuracy and the absence of essential parameters such as anticipation and asymmetric driving behavior when applied to human-driving and autonomous car-following planning.

During the last few years, some efforts have been made to capture the driving behavior of HD and AC vehicles in mixed traffic flow [44–47]. Some studies used the same car-following model [44, 45] to explore the driving behavior of HD and AC vehicles.

The effect of AC vehicles on stability traffic flow has been studied by Monteil et al. [45] to provide a new conception of AC vehicles application in the future using OVM and intelligent driver model (IDM) [22, 48].

Zhu and Zhang [44] used OVM to study the fundamental diagrams and density waves in mixed traffic flow. They established the bigger proportion of AC vehicles before the critical point of density-volume curve probably leads to a bigger volume in mixed traffic flow.

Some studies [46, 47] used different models to capture the driving behavior of HD and AC vehicles.

Yuan et al. [46] used a constant time headway (CTH) model and the modified comfortable driving (MCD) model for investigating the driving behavior of HD and AC vehicles on mixed traffic flow.

Yao et al. [47] conducted a developed full velocity difference (DFVD) model [49] and cooperative adaptive cruise control (CACC) to study the driving behavior of HD and AC vehicles in mixed traffic flow under different penetration rates of AC vehicles.

Table 2 focuses on HD and AC models and their related equations for mixed traffic flow within these studies [44–47].

The current studies have some deficiencies considering the HD and AC models and their impacts on mixed traffic flow characteristics.

First, most HD and AC models in these studies did not consider the motion information of several preceding vehicles. To our knowledge, AC and HD vehicles can receive motion information (e.g., velocity, position, and acceleration) from several preceding vehicles using wireless communication technology in automated highway systems.

Second, the impact of asymmetric and anticipation driving behavior has not been considered neither in human-driving traffic flow nor in mixed traffic flow as two main parts of driving.

Third, the environmental impacts (i.e., fuel consumption and emotion rates) of HD and AC models have not been investigated in these studies.

To overcome these deficiencies, we propose an asymmetric-anticipation full velocity difference (AAFVD) model to study the impacts of asymmetric characteristic and anticipation driving behavior on mixed traffic flow dynamics.

The remainder of the paper is organized as follows. We present the AAFVD model in Section 2. In Section 3, the linear stability analysis is conducted for the new model to study the qualitative properties of the AAFVD model. In Section 4, we analyze our model numerically under different scenarios of traffic flow. In Section 5, we evaluate the fuel consumption and exhaust emission rates of the AAFVD model during different situations of traffic flow. Concluding remarks are written in the last section.

2. The Car-following Model

2.1. Assumptions. We consider the operations of AC and HD vehicles, which are basically moving forward on a single-lane highway without any overtaking. The dynamic of mixed traffic flow is explained by the interactions between a small group of AC and HD vehicles at which AC vehicles will be controlled by the leader of the AC vehicles platoon. We derive our new car-following model equation based on the following assumptions [50]:

(i) There are two AC vehicles among two adjacent HD vehicles as depicted in Figure 1

(ii) Two AC vehicles are arranged in a closely spaced group denoted as platoon, which is moving along the roadway with the same velocity as their platoon leader

(iii) The vehicle inside the platoon accelerates only toward the optimal velocity of its leading vehicle

(iv) Each platoon is defined as a moving block according to platoon-based traffic operation in intelligent traffic systems (ITS)

(v) The following HD vehicle receives the motion information from its preceding platoon leader and its preceding HD vehicle in the communication range

(vi) Each platoon of AC vehicles follows a car-following behavior as same as the HD vehicle

2.2. An Asymmetric-Anticipation Full Velocity Difference Model. Among the existing car-following models, FVD model established by Jiang et al. [26] is one of the efficient car-following models. The existing studies show that FVD model enables to depict many complex phenomena in real traffic, such as shock waves, rarefaction waves, stop-and-go waves, and local cluster effects.

The FVD model can be formulated as follows:

$$\frac{\mathrm{d}v_n(t)}{\mathrm{d}t} = a\left[V_o\left(S_n(t)\right) - v_n(t)\right] + \lambda \Delta v_n(t), \tag{5}$$

where $S_n(t)$ is vehicular gap, $V_o(S_n(t))$ represents the optimal velocity function, $\Delta v_n(t)$ is relative velocity, and λ and a are sensitivity parameters.

The optimal velocity function is specified by $V_o(s_n(t)) = V_1 + V_2 \tan h(C_1(s_n(t) - lc) - C_2)$ with the following optimal parameter values:

Table 2: Summary of HD models, AC models, and equations for mixed traffic flow.

Reference	HD model	AC model	HD equation	AC equation
Zhu et al. [44]	OVM	OVM	$(\mathrm{d}v_n(t)/\mathrm{d}t) = a[V_o(S_n(t)) - v_n(t)]$	$(\mathrm{d}v_n(t)/\mathrm{d}t) = a[V_o(S_n(t), S_{n+1}(t)) - v_n(t)]$
Monteil et al. [45]	OVM	OVM	$(\mathrm{d}v_n(t)/\mathrm{d}t) = a[V_o(S_n(t)) - v_n(t)]$	$(\mathrm{d}v_n(t)/\mathrm{d}t) = a[V_o(\sum_{n=1}^{m} S_n(t)) - v_n(t)]$
	IDM	IDM	$(\mathrm{d}v_n(t)/\mathrm{d}t) = a_{\max}^n(1 - (v_n(t)/\overline{V}_n^d)^\beta - (\overline{S}_n^d/S_n(t)))^2,$	$(\mathrm{d}v_n(t)/\mathrm{d}t) = a_{\max}^n(1 - (v_n(t)/\overline{V}_n^d)^\beta - (\overline{S}_n^d/S_n(t)))^2$
Yuan et al. [46]	MCD	CTH	$x_{n+1}(t) = x_n(t) + v_n(t+1)$	$\tau(\mathrm{d}v_n(t)/\mathrm{d}t) = [V_o(S_n(t), \Delta v_n(t)) - v_n(t)]$
Yao et al. [47]	DFVD	CACC	$(\mathrm{d}v_n(t)/\mathrm{d}t) = a[V^*(S_n(t)) - v_n(t)] + (\lambda/S_n(t) - L)\Delta v_n(t)$	$(\mathrm{d}v_n(t)/\mathrm{d}t) = (k_p(S_n(t) - L - S_0) - k_p\overline{S}_n^d v_n(t) + k_d\Delta v_n(t)/k_d\overline{S}_n^d + \Delta t)$

Note: $V^*(S_n(t)) = v_{\text{free}}[1 - \exp(-(\alpha/v_{\text{free}})(S_n(t) - L - S_0))]$.

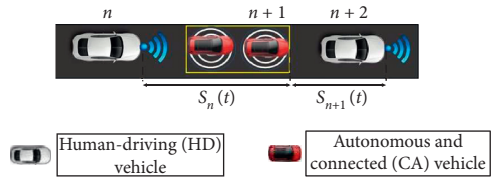

Figure 1: The mixed traffic flow including AC vehicles platoon and HD vehicles behavior.

$$\begin{aligned} V_1 &= 6.75\frac{m}{s}, \\ V_2 &= 7.91\ \frac{m}{s}, \\ C_1 &= 0.13\mathrm{m}^{-1}, \\ C_2 &= 1.57, \\ Lc &= 5\mathrm{m}. \end{aligned} \tag{5a}$$

In real-world traffic, the engine of vehicles has technical limitations during the acceleration process, which needs to be considered in a car-following model. In other words, when the relative velocity between two following and preceding vehicles enhances ($\Delta v_n \longrightarrow \infty$), the following vehicle cannot accelerate to infinity.

Therefore, the relation between acceleration and relative velocity is nonlinear in real traffic flow according to the actual experiments [29].

Building this observation and according to the actual experimental data [29], we add the exponential function to the FVD model as follows:

$$\frac{\mathrm{d}v_n(t)}{\mathrm{d}t} = a\left[V_o\left(S_n(t)\right) - v_n(t)\right] + \exp\left(-\mu\right)\Delta v_n(t)). \tag{5b}$$

Considering anticipation driving behavior, the motion information of preceding vehicles in connected vehicles environment, and the asymmetric characteristic of driving behavior due to the stimuli of relative velocities between the following HD vehicle and its two direct preceding vehicles (i.e., HD vehicle and AC vehicles platoon), we propose the dynamic equation of the AAFVD model as follows:

$$\begin{aligned} \frac{\mathrm{d}v_n(t)}{\mathrm{d}t} = a\big[&V_E\left(S_n, S_{n+1}, \Delta v_n, \Delta v_{n+1}\right) - v_n(t) \\ &+ \exp\left(-\mu\ \left((1-p)\Delta v_n(t) + p\Delta v_{n+1}(t)\right)\right) \\ &\left((1-p)\Delta v_n(t) + p\Delta v_{n+1}(t)\right)\big], \end{aligned} \tag{6}$$

$$\begin{aligned} V_E\left(S_n, S_{n+1}, \Delta v_n, \Delta v_{n+1}\right) &= (1-p)V_A\left(S_n(t) + T\Delta v_n(t)\right) \\ &+ pV_A\left(S_{n+1}(t) + T\Delta v_{n+1}(t)\right), \end{aligned} \tag{7}$$

where V_E is the expected optimal velocity of the following HD vehicle motion information of its direct preceding HD vehicle and AC platoon leader, T is forecast time, $T\left(\Delta v_n(t)\right)$ reflects the estimation of vehicular gap between the following HD vehicle (n) and its preceding platoon leader $(n+1)$, $T\Delta v_{n+1}(t)$ is the estimation of vehicular gap between the preceding platoon leader $(n+1)$ and the preceding HD vehicle $(n+2)$, p represents the weight effects of OV anticipation functions on the HD vehicle's reaction and is taken as $p \in [0, 0.3]$ since the influence of the first preceding vehicle is more important than the second preceding vehicle. $a = 0.6$ is the driver sensitivity parameter and $\mu = 0.2$ denotes an asymmetric constant [29]. The exponential function is the asymmetrical term that shows the driver's asymmetrical reaction regarding the relative velocities (Δv_n and Δv_{n+1}), also considering the realistic physical limitation of vehicle's acceleration when the relative velocity between the preceding and following vehicle is too big ($\Delta v_n \longrightarrow \infty, \Delta v_{n+1} \longrightarrow \infty$).

That is, when the velocity of the preceding vehicle is much bigger than the velocity of the following vehicle, therefore the vehicle cannot accelerate as much as the relative velocity increases considering engine technical limitations. It is in accordance with the empirical traffic data [29]; $S_n(t) = x_{n+1} - x_n$ denotes the vehicular gap between the following HD vehicle (n) and its preceding platoon leader $(n+1)$ at time step t; $S_{n+1}(t) = x_{n+2} - x_{n+1}$ represents the vehicular gap between the preceding HD vehicle $(n+2)$ and the preceding platoon leader $(n+1)$ at time step t; $\Delta v_n = v_{n+1} - v_n$ represents the relative velocity between the following HD vehicle (n) and the preceding platoon leader $(n+1)$ at time t; $\Delta v_{n+1} = v_{n+2} - v_{n+1}$ is the relative velocity between the preceding HD vehicle $(n+2)$ and the preceding platoon leader $(n+1)$ at time step t.

From equation (6), we can see that the OV anticipation functions of the following HD vehicle (n) and AC platoon leader $(n+1)$ are integrated into one synthesized OV anticipation function, and we can split it into two different OV anticipation functions using a linear combination method [51].

For later convenience of numerical simulations and linear analysis, we take the Taylor series expansion of equation (7) to the second order and ignore the higher orders, yielding the following equation:

$$\begin{aligned} V_A\left(S_n(t) + T\Delta v_n(t)\right) &= V_o\left(S_n(t)\right) + TV_o'\left(S_n(t)\right)\Delta v_n, \\ V_A\left(S_{n+1}(t) + T\Delta v_{n+1}(t)\right) &= V_o\left(S_{n+1}(t)\right) + TV_o'\left(S_{n+1}(t)\right)\Delta v_{n+1}. \end{aligned} \tag{8}$$

Thus, equation (7) can be written as follows:

$$\begin{aligned} V_A\left(S_n, S_{n+1}, \Delta v_n, \Delta v_{n+1}\right) &= (1-p)V_o\left(S_n(t)\right) + pV_o\left(S_{n+1}(t)\right) \\ &+ T\Delta v_n\left((1-p)V_o'\left(S_n(t)\right) + pV_o'\left(S_{n+1}(t)\right)\right). \end{aligned} \tag{9}$$

Putting equation (9) into equation (6), we will obtain

$$\begin{aligned}\frac{\mathrm{d}v_n(t)}{\mathrm{d}t} = a\big[&(1-p)V_o\big(S_n(t)\big) + pV_o\big(S_{n+1}(t)\big)\\ &+ T\Delta v_n\big((1-p)V_o'\big(S_n(t)\big) + pV_o'\big(S_{n+1}(t)\big)\big)\\ &- v_n(t) + \exp\big(-\mu\ \big((1-p)\Delta v_n(t) + p\Delta v_{n+1}(t)\big)\big)\\ &\big((1-p)\Delta v_n(t) + p\Delta v_{n+1}(t)\big)\big],\end{aligned} \tag{10}$$

where $V_o'(S_n(t)) = (\mathrm{d}V(S_n(t))/\mathrm{d}S_n(t))$ is the optimal velocity changing rate with vehicular gap and $V_o(S_n(t)), V_o(S_{n+1}(t))$ are OV functions, which are adopted as follows [25]:

$$\begin{aligned}V_o\big(S_n(t)\big) &= V_1 + V_2\tan h\big(\big(C_1\big(S_n(t)\big) - lc\big) - C_2\big),\\ V_o\big(S_{n+1}(t)\big) &= V_1 + V_2\tan h\big(\big(C_1\big(S_{n+1}(t)\big) - lc\big) - C_2\big),\end{aligned} \tag{11}$$

where the parameters are set as follows:

$$\begin{aligned}V_1 &= 6.75\frac{m}{s},\\ V_2 &= 7.91\frac{m}{s},\\ C_1 &= .13\mathrm{m}^{-1},\\ C_1 &= 1.57,\\ Lc &= 5\mathrm{m}.\end{aligned} \tag{12}$$

3. Linear Stability Analysis

The method of linear stability was first employed in the GHR model [48] by Chow [52]. Liu and Li [53] have evaluated the stability of a multiregime car following (CF) [54] via numerical simulation. Wilson and Ward [55] focused on classifying the analytical stability criterion of CF models with more details within a generalized frame.

To consider the impacts of anticipation and motion information from two direct preceding vehicles on mixed traffic flow stability, the method of linear stability is carried out to derive the stability and instability criteria for the AAFVD model.

We assume AC vehicles platoons and HD vehicles are distributed with the same vehicular gap (b) and are moving uniformly. Note that AC vehicles are moving much closer together because of the intelligent driving assistant system.

The optimal velocity of HD vehicles and AC vehicles platoon is $V(b,b)$. The position of each HD vehicle n in the stable traffic flow condition is as follows:

$$x_n^0(t) = bn + V_o(b,b)t, \quad n = 1, 2, \ldots, N, \tag{13}$$

where b is the vehicular gap denoted by $b = (D/N)$, N is the total number including platoons and HD vehicles, and D is the path distance.

By assuming that $y_n(t)$ stands for a slight deflection from the steady-status $x_n^0(t)$, i.e.,

$$x_n(t) = x_n^0(t) + y_n(t). \tag{14}$$

Equation (14) can be rewritten as follows:

$$y_n(t) = x_n(t) - x_n^0(t). \tag{15}$$

Equations (13) and (14) are replaced with a linear form of equation (10). The derived form of the asymmetrical function is $(1 - \exp(-\mu\ ((1-p)\Delta v_n(t) + p\Delta v_{n+1}(t))))\exp(-\mu\ ((1-p)\Delta v_n(t) + p\Delta v_{n+1}(t)))$, and the state of linear stability is autonomous from μ. The resulting equation yields

$$\begin{aligned}y_n''(t) = a\{&(1-p)\big(V_o'(b,b)\Delta y_n(t) + TV_o'(b,b)\Delta y_n'(t)\big) + p\big(V_o'(b,b)\Delta y_{n+1}(t) + TV_o'(b,b)\Delta y_{n+1}'(t)\big) - y_n'(t)\}\\ &+ \lambda\big((1-p)\Delta y_n'(t) + p\Delta y_{n+1}'(t)\big),\end{aligned} \tag{16}$$

where $V_o'(b) = (\mathrm{d}V(\Delta x_n)/\mathrm{d}\Delta x_n\|_{\Delta x_n=(1+p)b})$; $\Delta y_n(t) = \Delta x_n(t) - b$; $y_n'(t) = x_n'(t) - V_o(b,b)$; $y_n''(t) = x_n''(t)$, $\Delta y_{n+1}(t) = \Delta x_{n+1}(t) - b$; $\Delta y_n'(t) = \Delta x_n'(t)$; $\Delta y_{n+1}'(t) = \Delta x_{n+1}'(t)$; and β and λ are constants.

Expanding $y_n(t)$ into a Fourier series as an orthonormal set where $y_n(t) = e^{(i\alpha_k n + zt)}$, equation (10) can be defined by z as follows:

$$\begin{aligned}z^2 + [&a - \lambda\big((1-p)\big(\exp(i\alpha_k) - 1\big) + p\big(\exp(2i\alpha_k) - 1\big)\big) - TaV_o'(b,2b)\big((1-p)\big(\exp(i\alpha_k) - 1\big) + p\big(\exp(2i\alpha_k) - 1\big)\big)]z\\ &- aV_o'(b,2b)\big[(1-p)\big(\exp(i\alpha_k) - 1\big) + p\big(\exp(2i\alpha_k) - 1\big)\big] = 0.\end{aligned} \tag{17}$$

Inserting the expansion of $z = z_1(ik) + z_2(ik)^2 + \cdots$ into the above equation, the expressions of z_1 and z_2 are obtained as follows:

$$z_1 = V_o'(b,b)(1+p),$$
$$z_2 = \left(\frac{2\lambda(1+p)+a}{2a}\right)(1+p)V_o'(b,b) + \left(\frac{Ta-1}{a}\right)(1+p)^2\left(V_o'(b,b)\right)^2. \tag{18}$$

The uniform flow will remain stable provided if $z_2 > 0$ and unstable if $z_2 < 0$. So, the critical stable curve is given as

$$a_c = \frac{2(1+p)\left(V_o'(b,b)-\lambda\right)}{1+2T(1+p)V_o'(b,b)}. \tag{19}$$

Therefore, the stable and unstable regions are, respectively, as follows:

$$a_c > \frac{2(1+p)\left(V_o'(b,b)-\lambda\right)}{1+2T(1+p)V_o'(b,b)},$$
$$a_c < \frac{2(1+p)\left(V_o'(b,b)-\lambda\right)}{1+2T(1+p)V_o'(b,b)}. \tag{20}$$

If the first condition is satisfied, the AAFVD model is stable; otherwise, a collision or traffic congestion will happen as it propagates to upstream of traffic flow.

When $T = 0, p = 0$, the stable regions of the AAFVD model degrade to the stable regions of the FVD model [26].

Figure 2 illustrates the critical stability curves of the AAFVD and the FVD models in the parameter space $(\Delta x, a)$ under various amounts of T and p. In Figure 2, the solid red lines and the dashed blue lines represent the stability curves of AAFVD and the FVD models, respectively, and the apex of every curve defines the critical point (h_c, a_c) for various amounts of T and p, where h_c and a_c are, respectively, the safety distance and the critical sensitivity. The regions below the critical lines show the unstable regions where density waves appear in traffic flow, and the regions above the critical lines indicate the stable regions of traffic flow.

Figure 2 depicts that by incorporating the driving anticipation effect considering downstream motion information into the FVD model, the stable region gradually increases.

From Figure 2, it is clear that the stable region obtained from the AAFVD model is bigger than that obtained from the FVD model, and the critical points are significantly lower than the FVD model which means with increasing the impact of the driving anticipation the critical vehicular gap h_c will be smaller than that in the FVD model and the capacity of the road in the steady state will enhance.

4. Simulations

In this section, we perform the numerical simulations of the AAFVD model to support our new model by exploring the impacts of driving anticipation and asymmetric behavior and motion information from two preceding vehicles through V2V environment on velocity, acceleration, deceleration, energy consumption, exhaust emotions of HD vehicles and AC vehicles platoons, and the stability of mixed traffic flow under different traffic scenarios.

4.1. The Star-Up Process. Emulating the same scenario used by Jiang et al. [26], we analyze the departure process of HD and AC vehicles at a signalized intersection (Figure 3) to figure out the motion characteristics of each HD vehicle and AC vehicle platoon simulated by the AAFVD model.

We assume eleven vehicles (i.e., HD vehicles and AC vehicles platoons) stop in a queue during the red period of a traffic signal with identical vehicular gaps of 7.4 m at time $t < 0$. At time $t = 0$, the traffic signal shifts from its red period to its green period and the first preceding HD vehicle of mixed platoon instantly starts up, and the other vehicles gradually move and follow their direct preceding vehicle based on the AAFVD model in a connected system. The velocity of the first preceding HD vehicle and the AC vehicles platoon leader is defined by $v_{n+1} = v_{n+2} = v_0(t)$.

Figures 4(a)–4(d) depict how the following HD vehicle and the AC platoon duplicate fundamentally the velocity of preceding vehicles with a delay time, that is, $v_n = v_0(t - \delta t)$, in which δt is the delay time of each vehicle's motion. From the delay time of each vehicle's motion, we can further predict the velocity of kinematic waves (i.e., disturbance propagation velocity) at traffic jam with density c_j, which is defined by $c_j = 7.4/\delta t$.

Based on empirical observation, Bando et al. [24] found that the order of the delay time δt is 1 s; the range of the kinematic wave velocity was derived by Del Castillo and Benitez [56] to be between 17 and 23 km/h.

Comparing Figures 4(a) and 4(b), results revealed that the starting delay time of the following vehicles increases gradually when only the impact of asymmetric driving behavior is considered (i.e., anticipation and motion information from preceding vehicles are not considered) ($T = 0$, $p = 0$). In this case, the AAFVD model degrades to an asymmetric FVD model called AFVD model in our paper.

From Figures 4(c) and 4(d) and Table 3, it is clear that the following vehicles quickly respond to the change of the preceding vehicles, so the starting process of the following vehicles is getting faster because of receiving the motion information (i.e., position and velocity) from two preceding vehicles ($p = 0.3$), and anticipating the next moment of

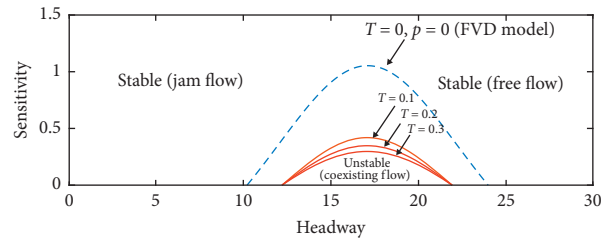

Figure 2: Phase diagram space of the AAFVD model in the parameter space $(\Delta x, a)$ according to various amounts of parameter (T) in $p = 0.3$.

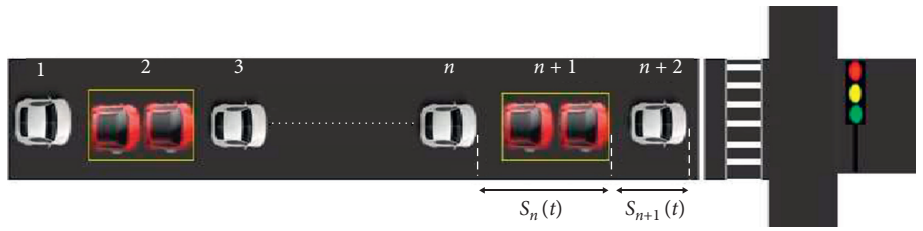

Figure 3: A mixed traffic flow platoon of eleven vehicles including AC vehicles platoon and HD vehicles proceeds as the traffic signal shifts from red to green.

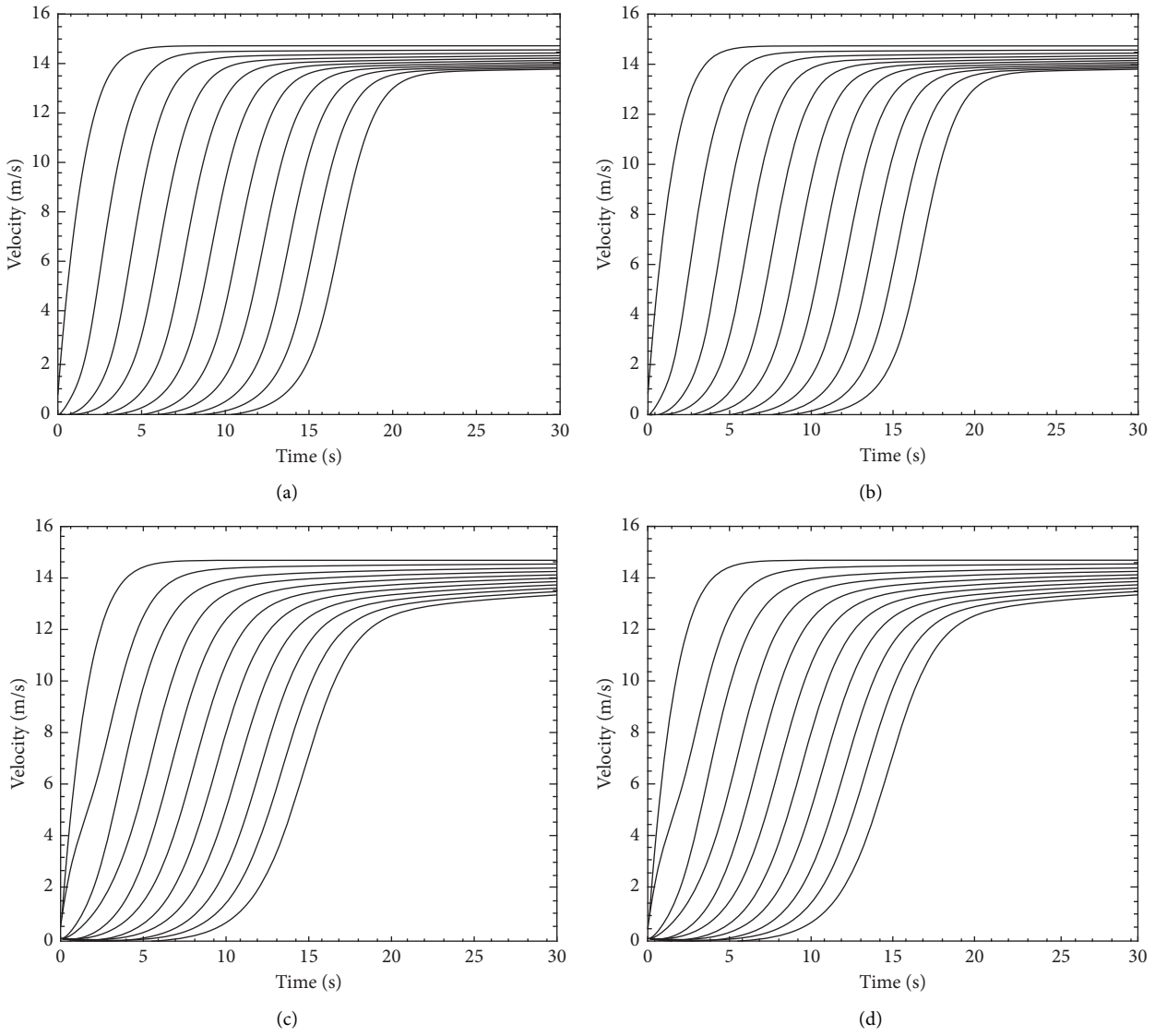

Figure 4: Motion of eleven vehicles during the departure process. (a) FVD model, (b) AFVD model ($T = 0$, $p = 0$), (c) AFVD model ($T = 0$, $p = 0.3$), and (d) AFVD model ($T = 0.1$, $p = 0.3$).

Table 3: Delay time δt (s) of vehicle motions in a signalized intersection and the velocity of kinematic wave (c_j) at traffic jam simulated by FDV and AAFVD models.

Model	a (1/s)	T (s)	p	δt (s)	c_j (km/h)
FVD	0.6	0	0	1.45	18.37
AFVD	0.6	0	0	1.5	17.8
AAFVD	0.6	0	0.3	1.39	19.16
AAFVD	0.6	0.1	0.3	1.30	20.49

downstream traffic situation ($T = 0.1$), the delay δt is getting shorter, and the velocity of kinematic wave c_j falls into in the defined boundary of observed data (17 km/h and 23 km/h). Such time-saving is critical for safety and operation.

To explore further how considering the anticipation and asymmetric driving behavior can affect the velocity and acceleration of the following vehicles in the V2V communication environment, we choose the 3rd vehicle and the 9th vehicle which both are HD vehicles to carry out a comparative analysis between the AAFVD, AFVD, and FVD models.

Figures 5(a), 5(b), 6(a), and 6(b), respectively, illustrate the velocity and acceleration evolution of the 3rd vehicle and 9th vehicle simulated by the FVD, AFVD, and AAFVD models with the value of $T = 0.1$, $p = 0.3$ and $p = 0$, $T = 0$.

In Figures 5(a) and 5(b), we can split the velocity of each target vehicle into two phases. During the first phase, the vehicle simulated by the AAFVD model accelerates faster than those simulated by the FVD and AFVD models.

In the second phase, the vehicle simulated by the AAFVD model accelerates slower than those simulated by the AFVD and FVD models.

Considering the above information, we can draw the conclusion that the vehicles simulated by the AAFVD model can accelerate faster due to the drivers' anticipation according to the received motion information from two preceding vehicles in connected vehicles environment and then accelerate smoothly until they reach the stable velocity.

During the second stage, drivers are relaxed in acceleration situation. However, those vehicles simulated by the AFVD and FVD models cannot behave in the same way. As a result, drivers can start moving forward instantly when the traffic signal shifts to green, higher acceleration can be avoided, and the vehicle's energy consumption can be reduced.

Figures 6(a) and 6(b) indicate that acceleration process can be split into two phases. In the first phase, the vehicle simulated by the AAFVD model applies the throttle pedal faster than one simulated by the AFVD and FVD models.

In the second phase, the vehicle simulated by the AFVD model and FVD model applies the throttle pedal faster than one simulated by the AAFVD model to reach the steady velocity. This benefits the following vehicles because they are interested to start applying the throttle pedal earlier to move forward faster when the traffic signal shifts to green to avoid a higher level of acceleration and then release the throttle pedal a little to feel safe until they reach a steady velocity.

Furthermore, from Figures 6(a) and 6(b), it is clear that the curves of the AAFVD model are lower than those of the AFVD and FVD models. The results demonstrate that the acceleration of vehicles simulated by the AAFVD model is within the limited range of empirical accelerations (0, 4) m/s^2 observed by Helbing and Tilch [25]. It means that the AAFVD model does not generate unrealistic high acceleration like the OV model [24].

By considering the impact of anticipation driving behavior, a driver can enhance his/her vehicle velocity more quickly and more gently. Therefore, efficiency and safety are improved in the starting process.

4.2. Braking Process. Here, the braking process of eleven vehicles is simulated numerically at a signalized intersection by using the AAFVD model under the initial conditions.

When $t < 0$, the traffic signal is green and eleven vehicles are moving forward with the same velocity of 4.66 (m/s); all vehicles are distributed uniformly with the same vehicular gap of 7.4 m on the road; the vehicular gap between the first preceding HD vehicle and the stopping line is supposed to be 10 m; the red light assumed to be a virtual vehicle with the velocity of zero at the stop line as noted in this literature [57].

At time $t = 0$, the traffic signal changes to red phase and the first preceding HD vehicle of the mixed platoon immediately brakes, and the following vehicles copy the first preceding HD vehicle's behavior with a delay time and begin to slow down gradually and all vehicles eventually will reach the velocity of zero before reaching the crosswalk.

The result of numerical simulation revealed that the following vehicles copy the velocity of the preceding vehicles with a delay time and eventually reach the velocity of zero in a queue before reaching the crosswalk, and the delay time of vehicles' motion simulated by the AAFVD, AFVD, and FVD models are 1.39 s, 1.5 s, and 1.43 s, respectively. It is clear that the AAFVD model has a shorter delay time than those of the AFVD and FVD models.

To investigate the impacts of anticipation and asymmetric driving behavior on the following vehicle's velocity during the braking process more clearly, we choose the 6th vehicle (i.e., platoon leader) and 9th vehicle (i.e., vehicle) as target vehicles.

The velocity evolution of two vehicles during the arrival process when vehicles start applying the brake pedal ($t = 0$) until that time both vehicles reach the velocity of zero in a queue before reaching the crosswalk is displayed in Figure 7 using the FVD, AFVD, and AAFVD models.

We can split the velocity of the 6th vehicle and 9th vehicle into two different phases in Figure 7; in the first phase, the following vehicles simulated by the AAFVD model start releasing the throttle pedal earlier and applying the brake pedal faster than those simulated by the AFVD and FVD models.

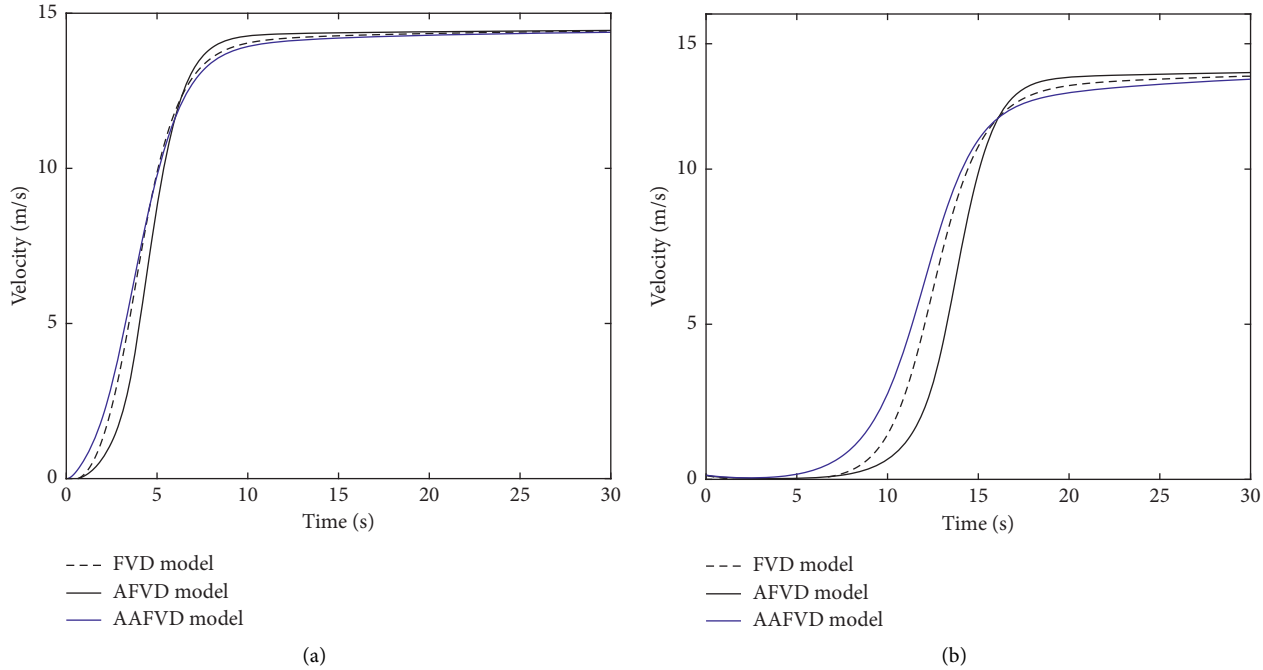

Figure 5: Velocities of two HD vehicles during the departure process simulated by the FVD, AFVD, and AAFVD models: (a) 3rd vehicle and (b) 9th vehicle.

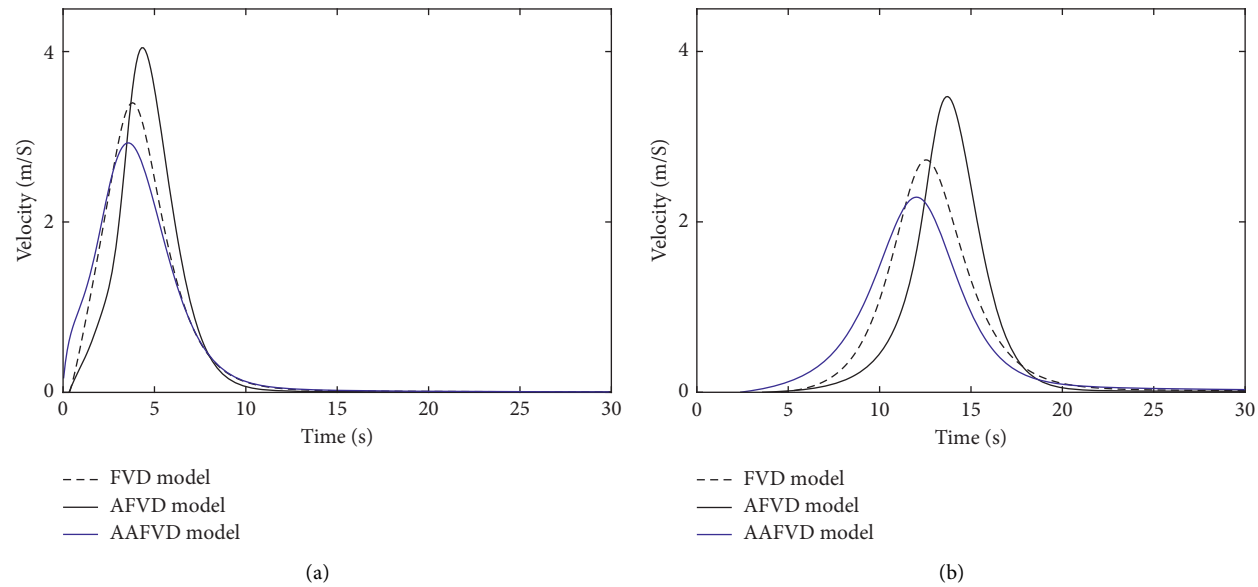

Figure 6: Acceleration of four HD vehicles during the departure process simulated by the FVD, AFVD, and AAFVD models: (a) 3rd vehicle and (b) 9th vehicle.

In the second phase, the following vehicles simulated by the AAFVD model reach the required amount of deceleration faster than those by the AFVD and FVD models until the vehicles stop completely.

In accordance with the above information, vehicles will be brought comfortably, gently, and safely to a standstill using the AAFVD model.

Figures 8(a)–8(c) depict the simulation of acceleration's evolution of eleven vehicles due to traffic signals using the FVD, AFVD, and AAFVD models, respectively. In this figure, the required level of deceleration in the AAFVD model is lower than that in the AFVD and FVD models and is not beyond the limited range of empirical deceleration $(-3, 4)$ (m/s^2) [25] observed from real driving behaviors.

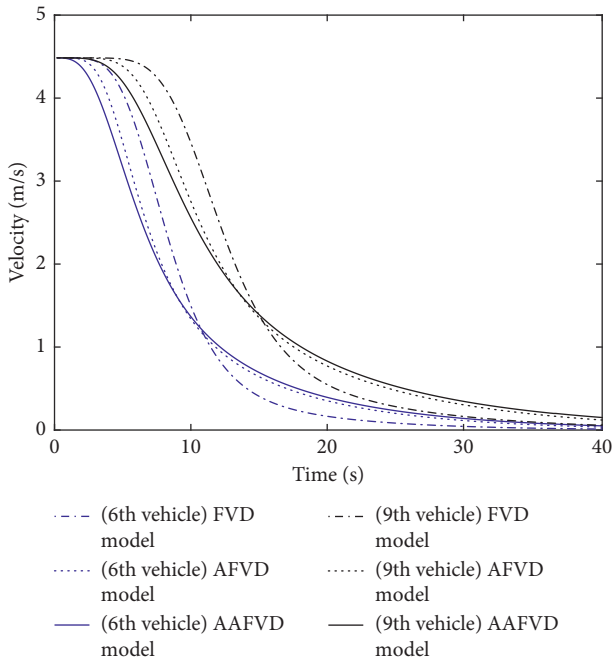

Figure 7: Comparison of two vehicles' velocity during the arrival process simulated by the FVD, AFVD, and AAFVD models.

To study more how receiving the motion information of two preceding vehicles can affect each vehicle's acceleration in a mixed platoon of vehicles during the arrival process, we select the 6^{th} vehicle and the 9^{th} vehicle to compare the AAFVD model with the above models. Figure 9 shows that the curve of the AAFVD model is in front of those of the AFVD and FVD models and is lower than those models.

Based on the above analysis, we can draw the conclusion that taking the motion information of two preceding vehicles into account in connected vehicles indeed has significant impacts on the evolution of each vehicle's acceleration. It enhances the capacity of signalized intersections.

4.3. Evolution Process with a Small Deflection. In this section, we investigate the effect of anticipation and asymmetric driving behavior on the stability of mixed traffic flow under an initial small deflection.

We will assume the mixed platoon of vehicles including HD vehicles and AC vehicles with the total number $N = 100$ which are moving forward uniformly along a circuit road with the path distance of $D = 1700$ m, under a periodic boundary condition (Figure 10). The initial state is set forth in the following equation:

$$x_1(0) = 1m; x_n(0) = \frac{n-1}{N} n \neq 1, \quad n = 2, 3, 4, \ldots\ldots, 100,$$
$$v_n(0) = V\left(\frac{D}{N}\right). \tag{21}$$

Figure 11 illustrates the snapshots of 100 vehicles' velocities simulated by the AAFVD model ($T = 0.1$, $p = 0.3$) and AFVD model ($T = 0$, $p = 0$) at $t = 300$ s, $t = 800$ s, and $t = 5000$ s.

It can be found from Figures 11(a)–11(c) that when anticipation of driving behavior considering two preceding vehicles motion information is taken into account, the amplitude of vehicles' velocity disappears after a short time.

All of these vehicles simulated by the AAFVD model move forward with a constant velocity $v_0 = 6.499$ (m/s) during 5000 s and the small initial deflection does not have a large effect on the stability of traffic flow. While we add a small initial deflection on vehicular traffic flow simulated by the AFVD model, it generates fluctuations around the constant velocity v_0 and the amplitude of vehicles' velocity fluctuates more by increasing time.

Jiang et al. [26] noted that the motion of the vehicles eventually begins to transit from a homogeneous phase to stop-and-go phase, which form into hysteresis loops after sufficient time.

In order to do further investigation, we show the hysteresis loop gained from the AAFVD model in three various scenarios. The first scenario is ignoring the anticipation driving behavior $T = 0$ and the effect of V2V communication theology on vehicles behavior $p = 0$ (i.e., AFVD model).

The second scenario is considering anticipation driving behavior without taking two preceding vehicles dynamic information into account in the V2V communication environment (i.e., $p = 0$, $T = 0.1$).

The third scenario is anticipating driving behavior with considering two preceding vehicles dynamic information in V2V environment which can be shown by $T = 0.1$ and $p = 0.3$ in the AAFVD model.

Figure 12 depicts that the traffic congestion stays unchanged after sufficient period of time. The motion of vehicles begins to form a loop of hysteresis phenomenon when drivers do not receive the motion information of two preceding vehicles $p = 0$ (i.e., AFVD model) and just anticipate the next moment of traffic flow based on their observation of next preceding vehicle's motion which is shown with $T = 0.1$ and $p = 0$.

From Figure 12, it is clear that the loop of the hysteresis phenomenon is getting smaller when the efficacy of anticipation on driving behavior increases. Furthermore, when we change the value of $T = 0$ and $p = 0$ to $T = 0.1$ and $p = 0.3$, we can see that the loop of hysteresis phenomenon does not form, and in the state space, there is only a point G on the OV line instead.

From Figure 12, two points can be noted as follows: first when $T = 0.1$ and $p = 0.3$, criterion (20) is held and the mixed traffic flow is stable and all vehicles run along the road with minimum gap which is 17 m. In other words, when $p = 0$ and $T = 0$ (AFVD model), a small part of the loop (point H) stands in the area, where the vehicular gap and velocity are less than the minimum amount of vehicular gap and velocity.

In summary, the above analysis of hysteresis loops and stop-go plots reveal that the AAFVD model provided superior results compared to the AFVD model. It clearly demonstrates that considering two preceding vehicles motion information using V2V communication technology can mitigate the appearance of traffic jams and enhance traffic

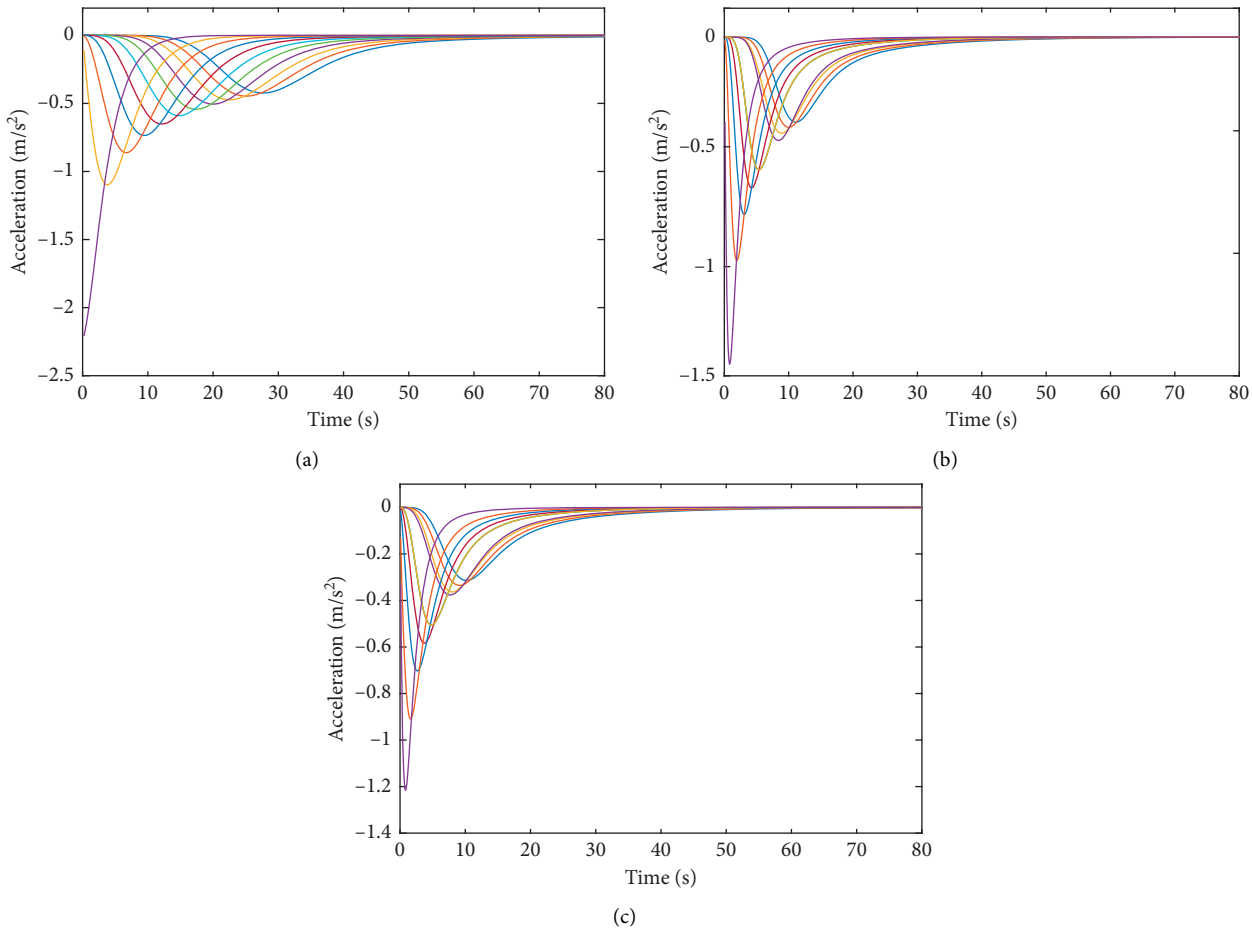

Figure 8: Acceleration evolution of eleven vehicles during the arrival process simulated by (a) FVD model, (b) AFVD model, and (c) AAFVD model.

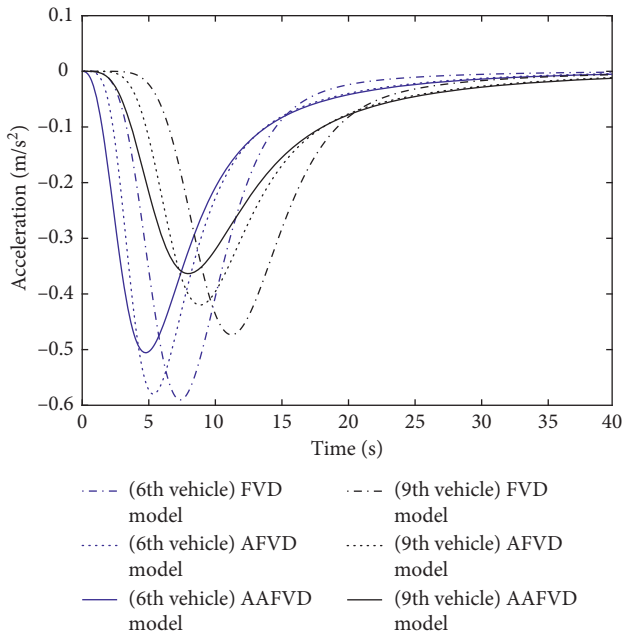

Figure 9: Comparison of two vehicles' acceleration during the arrival process simulated by the FVD, AFVD, and AAFVD models.

flow stability, which means that the velocity of vehicles changes sharply and the stop-and-go waves fluctuate smoothly. Driving smoothly means a low risk of traffic accidents. Therefore, we can draw the conclusion that driving safety is improved by considering the asymmetric-anticipation driving behavior.

5. Energy Consumption and Exhaust Emission Rates

The impacts of driving behavior on environment can be evaluated by vehicle energy consumption and exhaust emissions. Based on Ahn's model [58], Tang et al. [59] studied the energy consumption of each vehicle incorporating into three car-following models OVM [24], FVD [26], and FVAD [60] under various scenarios of traffic flow.

Rakha et al. [61] provided a trip-based microscopic traffic simulator INTEGRATION by incorporating VT-Micro model [58] to investigate how the energy consumption and exhaust emissions of vehicles are influenced by the ITS application and traffic light. Shi et al. [62] noted that the stability of the traffic flow has a significant effect on reducing the energy consumption of vehicles. Tang et al. [63] investigated the impacts of the real-time road state on

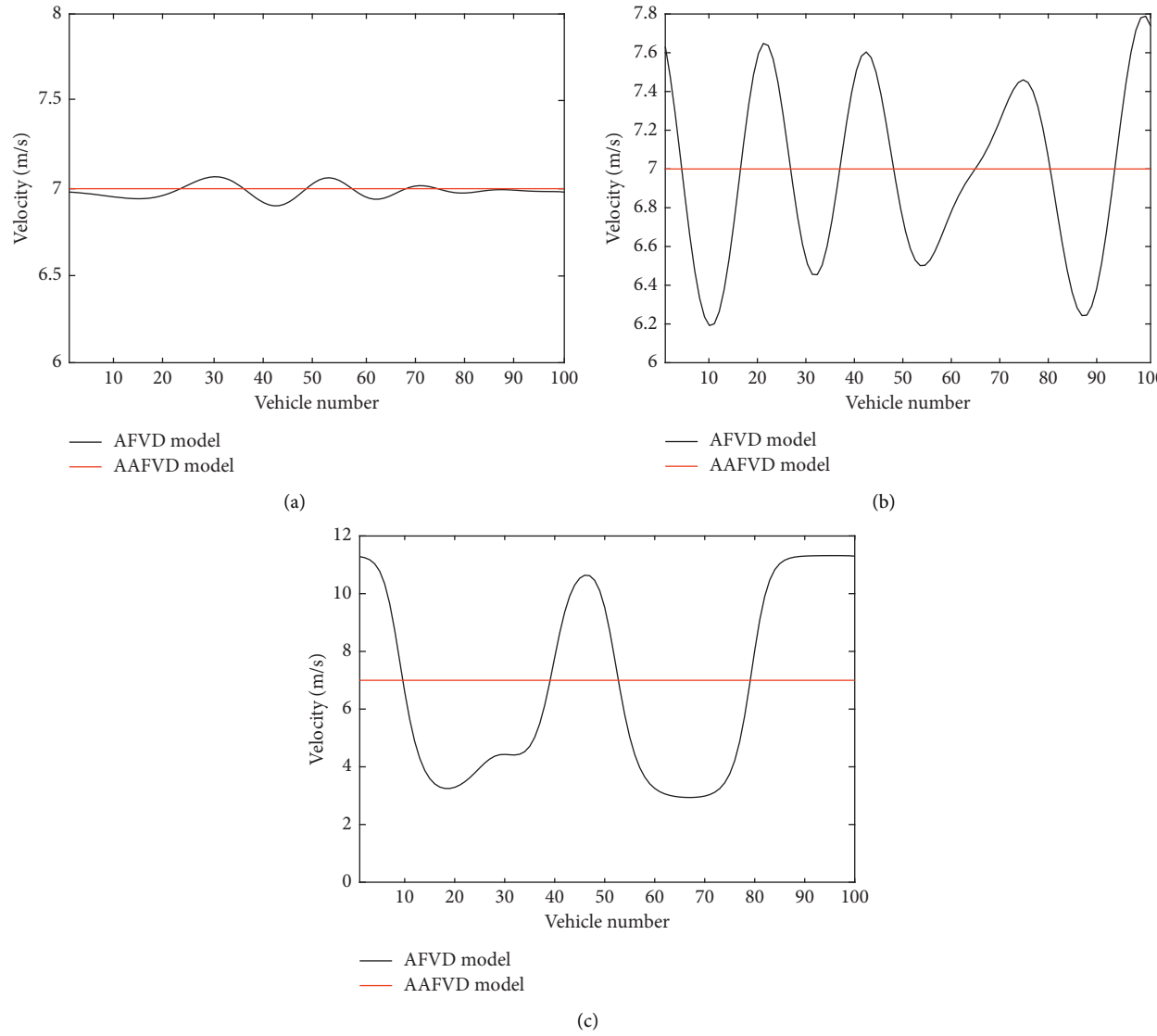

Figure 10: A mixed platoon of one hundred vehicles including CA vehicles platoon and HD driving vehicles moving forward on a circuit road with the path distance of $D = 1700$ m.

driving behavior, emissions (CO, HC, and NO_x), and energy consumption of vehicles in a new car-following model and confirmed that the stability of traffic flow affects vehicles' emissions and energy consumption.

Wu et al. [64] presented a new optimization system based on the idea of reducing vehicle's energy consumption and exhaust emission with modifying driving behavior. This system can help experienced and new drivers to adjust their acceleration/deceleration in accordance with traffic and environmental conditions as well as without violating any traffic rules.

The aforementioned studies showed how wise driving behavior can lead to lower exhaust emissions (CO, HC, and NO_x) and energy consumption. It is important to analyze the effects of anticipation driving behavior considering two leading vehicles motion information on exhaust emissions (CO, HC, and NO_x) and energy consumption of vehicles individually into our new model under different situations of traffic flow.

To evaluate the exhaust emissions (CO, HC, and NO_x) and energy consumption of an individual vehicle, we use the VT-Micro model (the Virginia Tech Microscopic energy and emission model) proposed by Ahn et al. [58] which reads

$$\ln(\text{MOE}e) = \sum_{i=0}^{i=3} \sum_{j=0}^{3} k_{i,j}^{e} * s^{i} * a^{j}, \tag{22}$$

where MOEe is the energy consumption rate (ml/s) or emission rate (mg/s) of an individual vehicle; $k_{i,j}^{e}$ is the coefficient of the regression model for MOE "e" at velocity power "i" and acceleration power "j" for negative accelerations which can be found in Appendix E in [65]; s is the instantaneous velocity; a is the instantaneous acceleration.

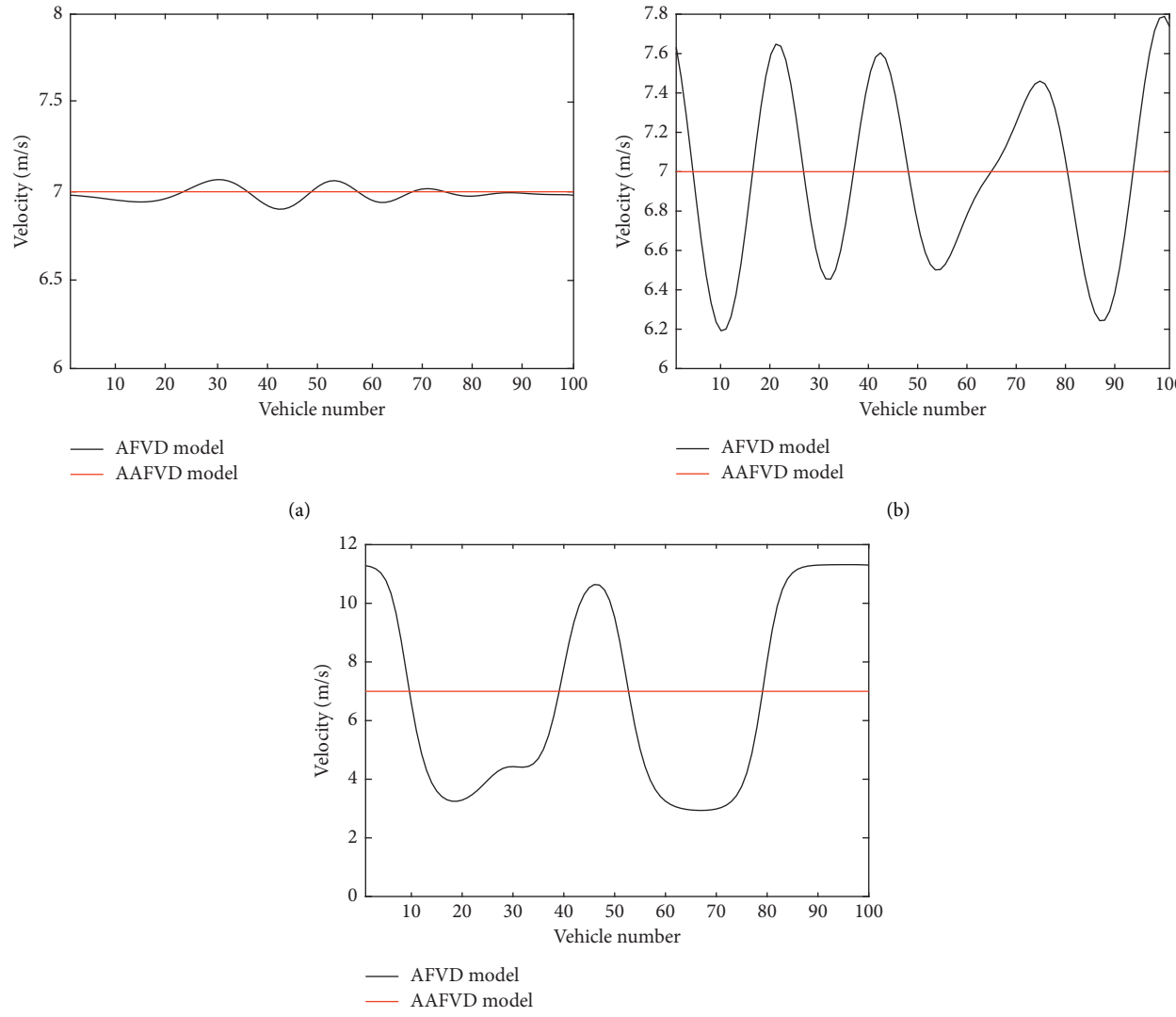

Figure 11: Snapshots of 100 vehicles' velocity simulated by the AFVD model ($T = 0$, $p = 0$) and the AAFVD model ($T = 0.1$, $p = 0.3$) at (a) 300 s, (b) 800 s, and (c) 5000 s.

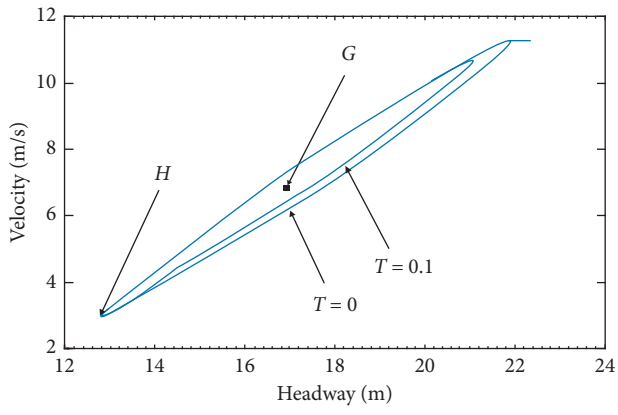

Figure 12: Hysteresis loops for the AAFVD model.

Figures 13–15 depict the instantaneous energy consumption and emission rates (CO, HC, and NO_x) of 10 vehicles by the AAFVD model during the departure and arrival processes under the following situation.

Ten vehicles are waiting in a queue with an identical vehicular gap of 7.4 m for the red period of a traffic signal which is situated at 74 m from 10^{th} vehicle; an obstacle is placed at 500 m from the last vehicle of the platoon. Other conditions are as same as the starting process in Section 4.1. When the obstacle appears, the first preceding vehicle of the platoon will start applying the brakes and then other vehicles duplicate this action. From Figures 13–17, we can observe the following results.

In Figure 13, we can split the energy consumption of each vehicle into four different phases during the departure and arrival process. In the first phase, drivers start pressing

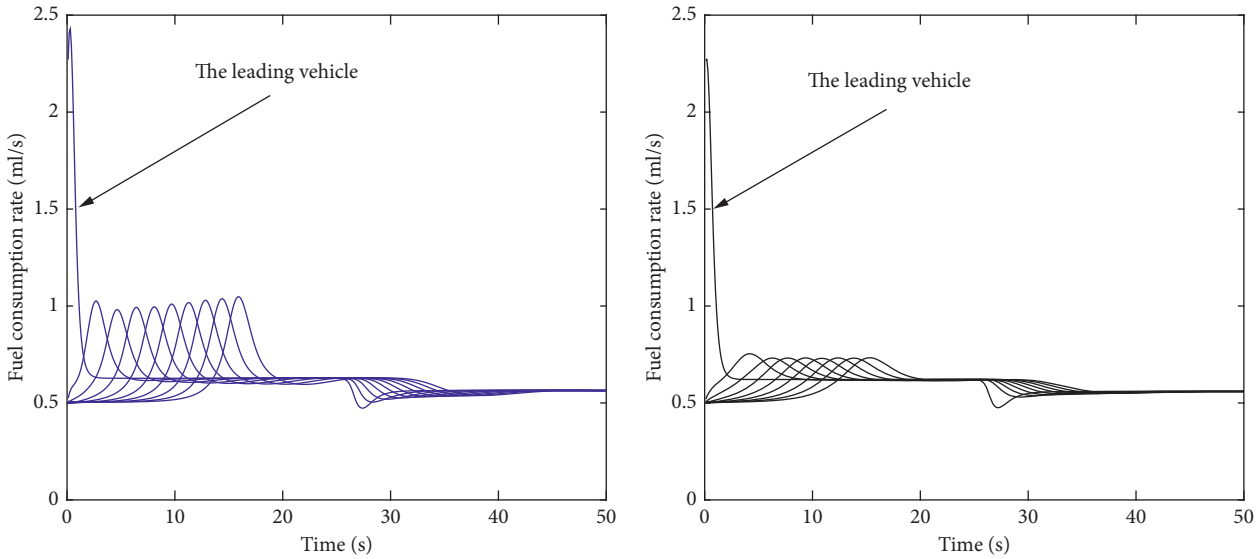

FIGURE 13: Fuel consumption of each vehicle during departure and arrival process simulated by the (a) AFVD model ($T = 0$, $p = 0$) and (b) AAFVD model ($T = 0.1$, $p = 0.3$).

the throttle pedal with high force to accelerate quickly and pass through the intersection during the green period of traffic signal, which leads to an enhancement of each vehicle's energy consumption.

In the second phase, drivers start releasing the throttle pedal because of reaching the required level of acceleration at the first phase, which reduces the acceleration and energy consumption of each vehicle.

In the third phase, drivers release the throttle pedal, but the velocity of each vehicle increases to its highest level and its acceleration to zero, which keeps the level of each vehicle's energy consummation constant.

In the fourth phase, a driver starts applying the brake pedal when finding out an obstacle in front; in this phase, the energy consumption of each vehicle slowly reduces as same as real traffic situation; however, the simulation process of energy consumption for each vehicle is very complex and irregular. It needs further exploration with some experiments in the future.

We can clearly see from Figures 13(a) and 13(b), the energy consumption of each vehicle reduces when the anticipation driving behavior is taken into account and the following vehicle receives the motion information of two preceding vehicles in the V2V communication environment ($T = 0.1$, $p = 0.3$).

From Figure 14, results revealed that the total fuel consumption of vehicles simulated by the AAFVD model reduced and HD drivers and CA platoon leaders can reply to the possible disturbances of downstream traffic carefully and unhurriedly.

From Figure 15, we can see that the total amount of CO is much more than the total amount of HC and NOx, but the total amount of CO, HC, and NO_x decreases when $T = 0.1$ and $p = 0.3$ because the acceleration process will become shorter in the AAFVD model. According to the vehicle's engine construction, during the acceleration process, an excessive amount of fuel will be injected into the vehicle's engine to avoid leaning the mixture too much and ensuring the engine runs without hitch. In other words, in the AAFVD model, the driver does not need to apply for a higher level of acceleration and release the throttle pedal to reach the velocity limit. By considering two preceding vehicles' motion information, the vehicle consumes less energy and reduces the emission rates.

Next, we determine the energy consumption rate and total exhaust emissions of first 50 vehicles of Section 4.3 under periodic boundary condition with a small deflection at the time step $t = 500$ s and $t = 1000$ s. All vehicles' energy consumption rate is illustrated in Figure 16.

From Figure 16, we can take the results as follows:

(i) When $T = 0$ and $p = 0$, vehicles' energy consumption produces oscillating phenomena because of the small deflection, and the small deflection will not be dissipated during 1000 s.

(ii) When $T = 0.1$ and $p = 0.3$, the energy consummation of each vehicle is stable because CA and HD vehicles can adjust their movement earlier by anticipating the next moment of traffic situation and receiving downstream traffic information in V2V environment, causing drivers to avoid applying for unnecessary brake or accelerator pedals.

Figures 17(a)–17(c) depict the total amount of CO, HC, and NO_x emission of 50 vehicles simulated by the AAFVD model with different values of $T = 0$, $p = 0$, and $T = 0.1$, $p = 0.3$ at the time step of 1000 s.

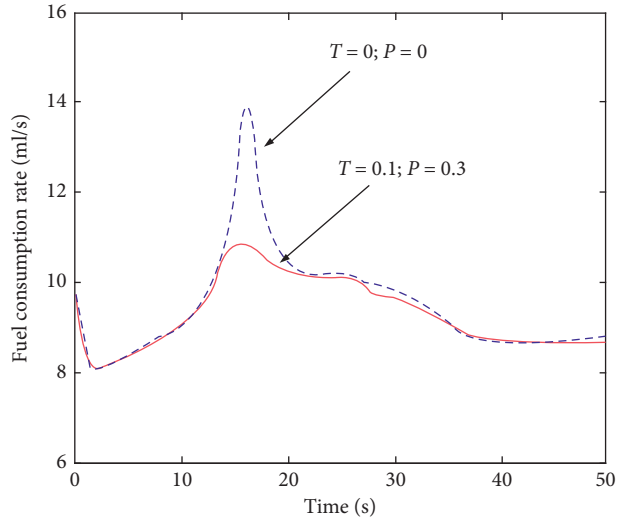

FIGURE 14: Total fuel consumption of each vehicle during departure and arrival process simulated by the AFVD model ($T = 0$, $p = 0$), the AAFVD model ($T = 0.1$, $p = 0.3$).

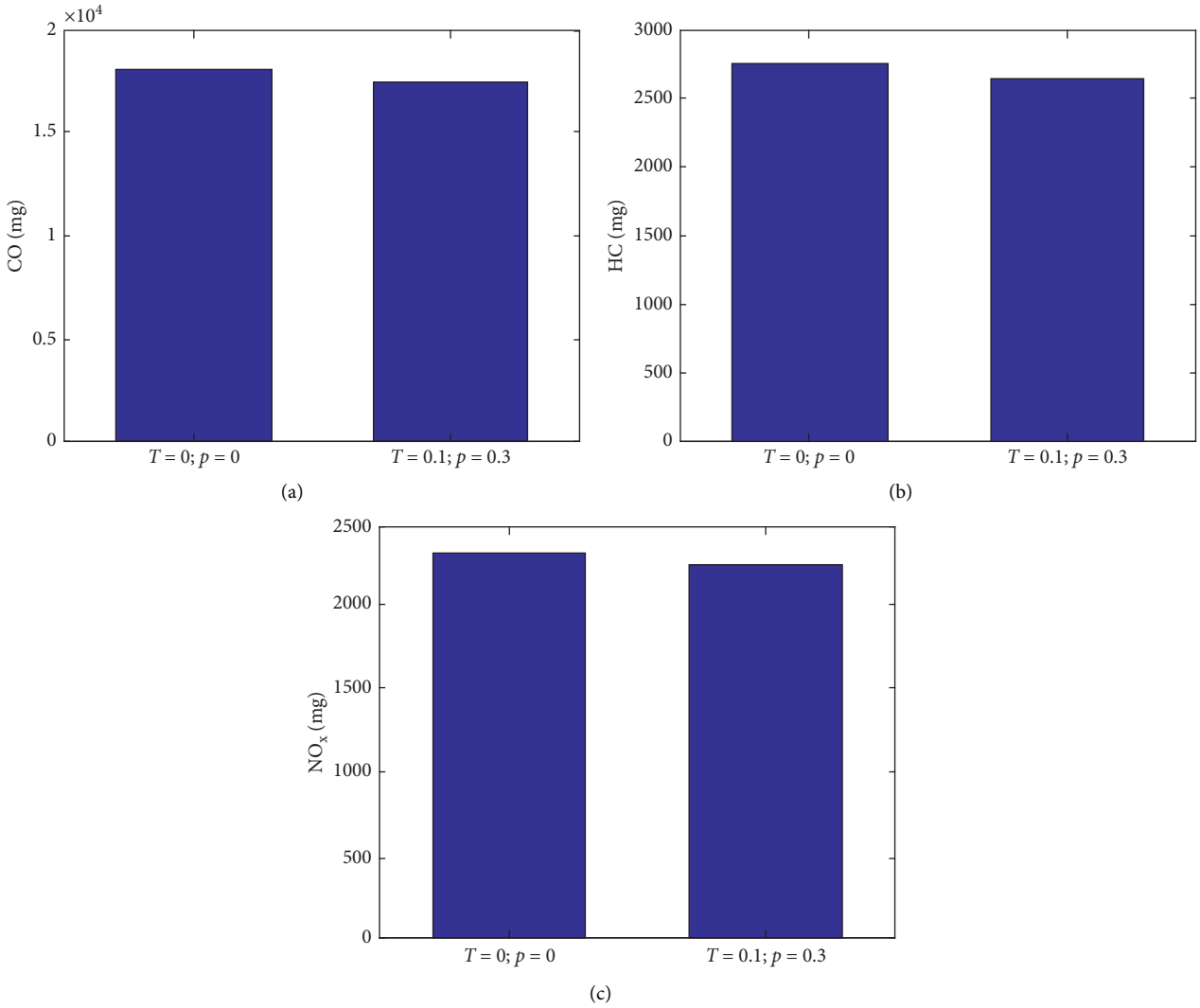

FIGURE 15: The total CO, HC, and NO_x emission of 10 vehicles simulated by the AFVD model ($T = 0$, $p = 0$) and the AAFVD model ($T = 0.1$, $p = 0.3$) during departure and arrival process: (a) CO, (b) HC, and (c) NO_x.

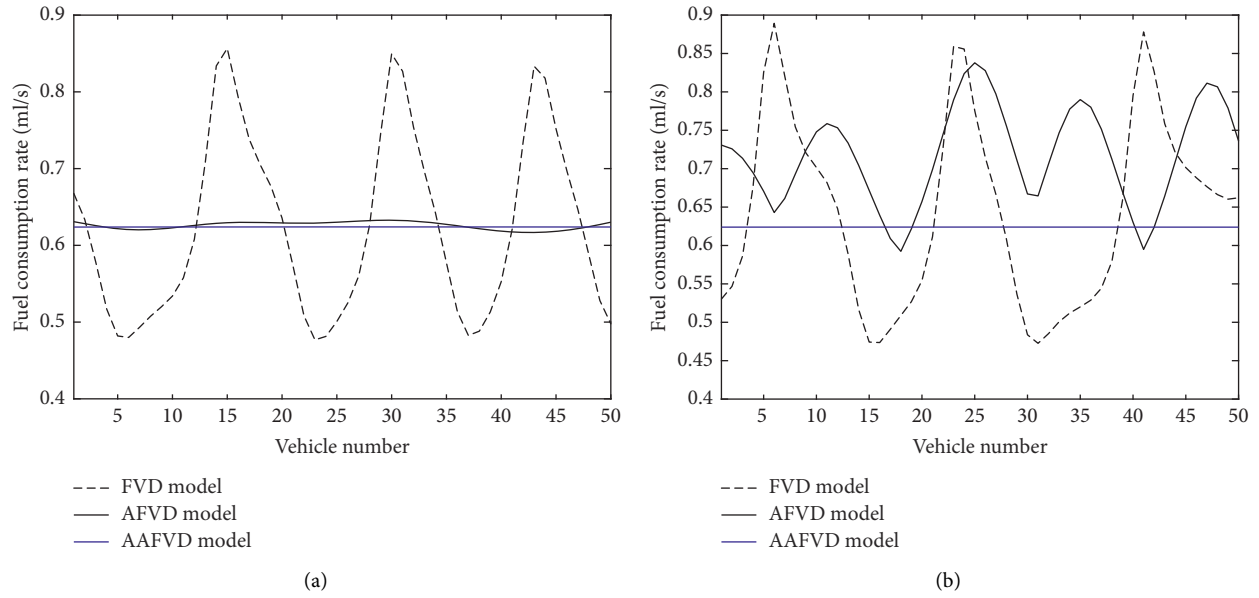

Figure 16: Snapshots of energy consumption rate of 50 vehicles simulated by the FVD model, AFVD model ($T = 0$, $p = 0$), and AAFVD model ($T = 0.1$, $p = 0.3$) at time step (a) 500 s and (b) 1000 s.

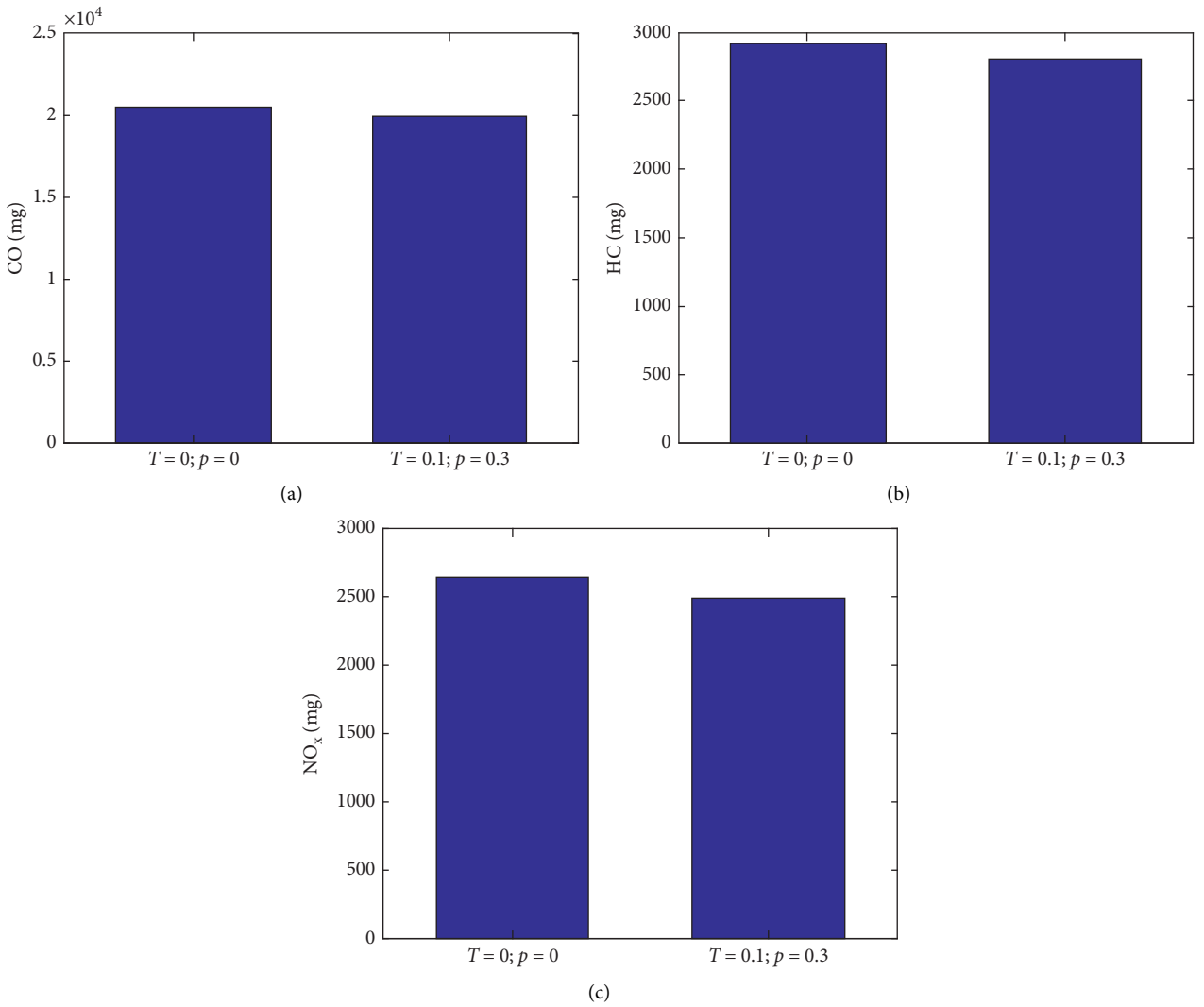

Figure 17: The total CO, HC, and NO_x emission of 50 vehicles simulated by simulated by the AFVD model ($T = 0$, $p = 0$) and the AAFVD model ($T = 0.1$, $p = 0.3$) at time step 1000 s: (a) CO, (b) HC, and (c) NO_x.

From Figures 17(a)–17(c), we can see the total amount of CO is much more than the total amount of HC and NO_x, but the total amount of CO, HC, and NO_x under the value of $T = 0.1$, $p = 0.3$ is lower than that under the value of $T = 0$, $p = 0$.

6. Concluding Remarks

To contribute to the state of the art in traffic flow theory, we proposed the AAFVD model based on the FVD model with an anticipation optimal velocity function considering the reflection of vehicular gap and velocity changes of two preceding vehicles using the V2V communication technology.

The asymmetrical term was added to take the realistic physical limitation of vehicle acceleration into account to make the AAFVD model more realistic according to real traffic situations in ITS systems.

Linear stability analysis was conducted to study on traffic flow characteristics.

We experimented our numerical simulations for evaluating the efficiency of the AAFVD model in the starting process, taking process, small deflections, and vehicle's emission and fuel consumption rate.

Our results revealed that high acceleration and deceleration will not appear, and considering the anticipation driving behavior for designing the control strategy of mixed traffic systems can increase positive traffic metrics (safety and flow) and decrease energy consumption and CO, HC, and NO_x emissions.

Considering the anticipation driving behavior according to the motion information of two preceding vehicles enhances the stability of traffic flow by eliminating unnecessary-dangerous interactions among vehicles, achieves a better traffic flow in terms of safety, and reaches a better condition for traffic flow to operate.

The results depict that the AAFVD model can more successfully anticipate the two important traffic parameters comparing with the FVD model: the delay time of vehicle motion and the kinematic wave speed at jam density. It means that efficiency and safety can be improved in signalized intersection by considering the effect of the asymmetric-anticipation driving behavior according to motion information of two preceding vehicles.

The AAFVDM model enhances our capability to analyze not only a single preceding vehicle but also the entire ambient traffic conditions in the vicinity of the subject vehicle. This can be implemented accurately through V2V wireless communication.

The results showed that the degraded model, which is derived from the AAFVD model (i.e., AFVD model), exhibited good agreement with manual driving systems compared to the FVD model. This is due to considering the asymmetric driving behavior.

We did not consider the memory of driving, bounded rationality, and the downstream traffic condition in our proposed model, which have significant influences on car-following behavior.

Another limitation of our paper is that we do not use some experimental real data to testify numerical results.

The results obtained in this paper are qualitative. Therefore, more efforts will be done in our future work to combine many observed data to further study the inner relationship between the AAFVD model and the stability of traffic flow.

We are currently undertaking an ongoing investigation which calibrates empirically our new model using real traffic data. The result of calibration can help us to realize quantitatively the impact of anticipation and asymmetric driving behavior on microscopic traffic flow.

However, more studies are required to be conducted to analyze the applicability of our new microscopic model to real traffic systems, and it may be rational to result that it affords an accurate description of traffic flow.

Abbreviations

CF: Car following
FVD: Full velocity difference model
IDM: Intelligent driver model
OVM: Optimal velocity model
OV: Optimal velocity
AC: Autonomous and connected
HD: Human driving
ITS: Intelligent transportation system
ICT: Information and communication technologies
V2V: Vehicle-to-vehicle
CA: Cellular automata
GFM: General Ford model
TVD: Two-velocity difference
MCD: Modified comfortable driving
CTH: Constant time headway
DFVD: Developed full velocity difference
CACC: Adaptive cruise control
AFVD: Asymmetric full velocity difference
AAFVD: Anticipation-asymmetric full velocity difference
$x_n(t)$: The position of the nth HD vehicle at time t
$v_n(t)$: Velocity of the nth HD vehicle at time t
$a_n(t)$: The acceleration (deceleration) of nth HD vehicle
$S_n(t)$: The vehicular gap between AC platoon leader $n+1$ and the following HD vehicle n at time t, $S_n(t) = \Delta x_n(t) = x_{n+1}(t) - x_n(t)$
$S_{n+1}(t)$: The vehicular gap between the preceding HD vehicle $n+2$ and the AC platoon leader $n+1$ at time step t, $S_{n+1}(t) = \Delta x_{n+1}(t) = x_{n+2}(t) - x_{n+1}(t)$
$\Delta v_n(t)$: The relative velocity between the AC platoon leader $n+1$ and the following HD vehicle n at time step t, $\Delta v_n(t) = v_{n+1}(t) - v_n(t)$
$\Delta v_{n+1}(t)$: The relative velocity between the preceding HD vehicle $n+2$ and the AC platoon leader $n+1$ at time step t, $\Delta v_{n+1}(t) = v_{n+2}(t) - v_{n+1}(t)$
$\overline{V}_n^d$: The desired velocity
$\overline{V}_E$: The following HD vehicle's expected optimal velocity
τ_n: The reaction time

$T\Delta v_n(t)$: The following HD vehicle's estimation of the vehicular gap between AC platoon leader $n+1$ and following HD vehicle n at the next moment
$T\Delta v_{n+1}(t)$: The following HD vehicle's estimation of the vehicular gap between vehicles $n+2$ and $n+1$ at the next moment
V_O: The optimal velocity function
V_E: The expectation of optimal velocity
V_A: The anticipation function of optimal velocity
$V_e(\rho)$: Equilibrium velocity
a: The sensitivity of the driver given by the inverse of the delay time of vehicle motion τ, namely, $a = 1/\tau$
λ: The sensitive constant
p: The weight parameter
a_n: The considered vehicle's acceleration at the time step t
H: The Heaviside step function
T: The forecast time
δt: The vehicle's delay time during departure and arrival process
c_j: The velocity of the kinematic wave at traffic jam, equal to the quotient of the vehicular gap divided by the vehicle's delay time δt; $c_j = S/\delta t$
μ: The asymmetric factor
a_c: The stability function of the microscopic model
α_k: Set of the eigenmodes
$d_{n(\text{effective})}$: Effective distance
$v_{\text{anti}}(t)$: Anticipated velocity of preceding vehicle in next moment
$\overline{S}_n^d$: The desired vehicular gap
$\overline{V}_n^d$: The desired velocity
L: The vehicle length
v_{free}: Free flow velocity
k_p, k_d: Control parameters
S_0: Minimum safe distance.

Data Availability

The data published in this paper can be available and accessible from the corresponding author upon written official request with legitimate justification.

Additional Points

An asymmetric-anticipation full velocity difference (AAFVD) car-following model was proposed. The AAFVD model takes the effects of the anticipation and asymmetric driving behavior and two preceding vehicles' motion information into account. The AAFVD model improves the stability of mixed traffic flow. The AAFVD model reduces the vehicle's energy consumption and exhaust emissions of CO, NO_x, and HC.

Conflicts of Interest

The authors declare that they have no conflicts of interest.

Acknowledgments

This study was supported in part by China Scholarship Council, the National Natural Science Foundation of China under grants 41574022, 51250110075, U1134206, and 51050110143 and the American Association of Highway and Transportation Officials under grant 15-0084 to which the authors are very grateful.

References

[1] S. Ilgin, M. Menendez, and L. Meier, "Using connected vehicle technology to improve the efficiency of intersections," *Transportation Research Part C*, vol. 46, pp. 121–131, 2014.
[2] J. Noah, B. Smith, and B. Park, "Traffic signal control with connected vehicles," *Journal of the Transportation Research Board*, vol. 15, 2012.
[3] E. Uhlemann, "The US and Europe advances V2V deployment [connected vehicles]," *IEEE Vehicular Technology Magazine*, vol. 12, no. 2, pp. 18–22, 2017.
[4] A. Bazzi, B. M. Masini, A. Zanella, and I. Thibault, "On the performance of IEEE 802.11p and LTE-V2V for the cooperative awareness of connected vehicles," *IEEE Transactions on Vehicular Technology*, vol. 66, no. 11, pp. 10419–10432, 2017.
[5] K. C. Dey, A. Rayamajhi, M. Chowdhury, P. Bhavsar, and J. Martin, "Vehicle-to-vehicle (V2V) and vehicle-to-infrastructure (V2I) communication in a heterogeneous wireless network-performance evaluation," *Transportation Research Part C: Emerging Technologies*, vol. 68, pp. 168–184, 2016.
[6] D. J. Fagnant, K. M. Kockelman, and P. Bansal, "Operations of shared autonomous vehicle fleet for Austin, Texas, market," *Transportation Research Record*, vol. 2536, pp. 98–106, 2015.
[7] W. Do, O. M. Rouhani, and L. M. Moreno, "Simulation-based connected and automated vehicle models on highway sections: a literature review," *Journal of Advanced Transportation*, vol. 2019, Article ID 9343705, 14 pages, 2019.
[8] P. Bansal and K. M. Kockelman, "Forecasting Americans' long-term adoption of connected and autonomous vehicle technologies," *Transportation Research Part A: Policy and Practice*, vol. 95, pp. 49–63, 2017.
[9] M. Campbell, M. Egerstedt, J. P. How, and R. M. Murray, "Autonomous driving in urban environments: approaches, lessons and challenges," *Philosophical Transactions of the Royal Society A: Mathematical, Physical and Engineering Sciences*, vol. 368, no. 1928, pp. 4649–4672, 2010.
[10] A. Broggi, P. Cerri, M. Felisa, M. C. Laghi, L. Mazzei, and P. P. Porta, "The vislab intercontinental autonomous challenge: an extensive test for a platoon of intelligent vehicles," *International Journal of Vehicle Autonomous Systems*, vol. 10, no. 3, pp. 147–164, 2012.
[11] E. Aria, J. Olstam, and C. Schwietering, "Investigation of automated vehicle effects on driver's behavior and traffic performance," *Transportation Research Procedia*, vol. 15, pp. 761–770, 2016.
[12] A. Olia, S. Razavi, B. Abdulhai, and H. Abdelgawad, "Traffic capacity implications of automated vehicles mixed with regular vehicles," *Journal of Intelligent Transportation Systems*, vol. 22, no. 3, pp. 244–262, 2018.
[13] A. Jafaripournimchahi, W. Hu, and L. Sun, "Nonlinear stability analysis for an anticipation-memory car following model in the era of autonomous and connected vehicles," in *Proceedings of the 2020 International Conference On Urban*

Engineering and Management Science (ICUEMS), pp. 409–413, Zhuhai, China, March 2020.

[14] J. Sun, Z. Zheng, and J. Sun, "Stability analysis methods and their applicability to car-following models in conventional and connected environments," *Transportation Research Part B: Methodological*, vol. 109, pp. 212–237, 2018.

[15] D. Xie, X. Zhao, and Z. He, "Heterogeneous traffic mixing regular and connected vehicles: modeling and stabilization," *IEEE Transactions on Intelligent Transportation Systems*, vol. 20, pp. 1–12, 2018.

[16] Y. Qin, H. Wang, and B. Ran, "Stability analysis of connected and automated vehicles to reduce fuel consumption and emissions," *Journal of Transportation Engineering, Part A: Systems*, vol. 144, 2018.

[17] L. Sun, A. Jafaripournimchahi, and W. Hu, "Driver's anticipation and memory driving car-following model," *Journal of Advanced Transportation*, vol. 2020, Article ID 4343658, 2020.

[18] L. Ye and T. Yamamoto, "Modeling connected and autonomous vehicles in heterogeneous traffic flow," *Physica A: Statistical Mechanics and Its Applications*, vol. 490, pp. 269–277, 2018.

[19] R. E. Chandler, R. Herman, and E. W. Montroll, "Traffic dynamics: studies in car following," *Operations Research*, vol. 6, no. 2, pp. 165–184, 1958.

[20] R. Herman, E. W. Montroll, R. B. Potts, and R. W. Rothery, "Traffic dynamics: analysis of stability in car following," *Operations Research*, vol. 7, no. 1, pp. 86–106, 1959.

[21] D. C. Gazis, R. Herman, and R. W. Rothery, "Nonlinear follow-the-leader models of traffic flow," *Operations Research*, vol. 9, no. 4, pp. 545–567, 1961.

[22] M. Treiber, A. Hennecke, and D. Helbing, "Congested traffic states in empirical observations and microscopic simulations," *Physical Review E*, vol. 62, no. 2, pp. 1805–1824, 2000.

[23] G. F. Newell, "Instability in dense highway traffic, a review," in *Proceedings of the Second International Symposium on the Theory of Traffic Flow*, pp. 73–85, London, UK, June 1965.

[24] M. Bando, K. Hasebe, K. Nakanishi, and A. Nakayama, "Analysis of optimal velocity model with explicit delay," *Physical Review E*, vol. 58, no. 5, pp. 5429–5435, 1998.

[25] D. Helbing and B. Tilch, "Generalized force model of traffic dynamics," *Physical Review E*, vol. 58, no. 1, pp. 133–138, 1998.

[26] R. Jiang, Q. Wu, and Z. Zhu, "Full velocity difference model for a car-following theory," *Physical Review E*, vol. 64, p. 017101, 2001.

[27] H. X. Ge, R. J. Cheng, and Z. P. Li, "Two velocity difference model for a car following theory," *Physica A: Statistical Mechanics and its Applications*, vol. 387, pp. 5239–5245, 2008.

[28] H. Gong, H. Liu, and B.-H. Wang, "An asymmetric full velocity difference car-following model," *Physica A: Statistical Mechanics and Its Applications*, vol. 387, no. 11, pp. 2595–2602, 2008.

[29] D. Shamoto, A. Tomoeda, R. Nishi, and K. Nishinari, "Car-following model with relative-velocity effect and its experimental verification," *Physical Review E*, vol. 83, no. 4, 046105 pages, 2011.

[30] J. Zhao, V. L. Knoop, and M. Wang, "Two-dimensional vehicular movement modelling at intersections based on optimal control," *Transportation Research Part B: Methodological*, vol. 138, pp. 1–22, 2020.

[31] J. Zhao, J. O. Malenje, J. Wu, and R. Ma, "Modeling the interaction between vehicle yielding and pedestrian crossing behavior at unsignalized midblock crosswalks," *Transportation Research Part F: Traffic Psychology and Behaviour*, vol. 73, pp. 222–235, 2020.

[32] T.-Q. Tang, Z.-Y. Yi, J. Zhang, T. Wang, and J.-Q. Leng, "A speed guidance strategy for multiple signalized intersections based on car-following model," *Physica A: Statistical Mechanics and Its Applications*, vol. 496, pp. 399–409, 2018.

[33] D. Ngoduy, "Linear stability of a generalized multi-anticipative car following model with time delays," *Communications in Nonlinear Science and Numerical Simulation*, vol. 22, no. 1–3, pp. 420–426, 2015.

[34] L. Sun, A. Jafaripournimchahi, and W. Hu, "A forward-looking anticipative viscous high-order continuum model considering two leading vehicles for traffic flow through wireless V2X communication in autonomous and connected vehicle environment," *Physica A: Statistical Mechanics and Its Applications*, vol. 556, p. 124589, 2020.

[35] S. Yu, J. Tang, and Q. Xin, "Relative velocity difference model for the car-following theory," *Nonlinear Dynamics*, vol. 91, no. 3, pp. 1415–1428, 2018.

[36] Y. Guo, Y. Xue, Y. Shi, F.-p. Wei, H. D. He., and L.-z. Lü, "Mean-field velocity difference model considering the average effect of multi-vehicle interaction," *Communications in Nonlinear Science and Numerical Simulation*, vol. 59, pp. 553–564, 2018.

[37] D. Sun, D. Chen, M. Zhao, W. Liu, and L. Zheng, "Linear stability and nonlinear analyses of traffic waves for the general nonlinear car-following model with multi-time delays," *Physica A: Statistical Mechanics and Its Applications*, vol. 501, pp. 293–307, 2018.

[38] L. Sun, A. Jafaripournimchahi, A. Kornhauser, and W. Hu, "A new higher-order viscous continuum traffic flow model considering driver memory in the era of autonomous and connected vehicles," *Physica A: Statistical Mechanics and Its Applications*, vol. 547, p. 123829, 2020.

[39] S.-W. Yu and Z.-K. Shi, "An improved car-following model with two preceding cars' average speed," *International Journal of Modern Physics C*, vol. 26, no. 8, p. 1550094, 2015.

[40] L. J. Zheng and C. Tian, D. H. Sun, W. N. Liu, A new car-following model with consideration of anticipation driving behavior," *Nonlinear Dynamic*, vol. 70, pp. 1205–1211, 2012.

[41] T. Q. Tang, C. Y. Li, and H. J. Huang, "A new car-following model with the consideration of the driver's forecast effect," *Physics Letters A*, vol. 374, no. 38, pp. 3951–3956, 2010.

[42] G. Peng, "A new lattice model of the traffic flow with the consideration of the driver anticipation effect in a two-lane system," *Nonlinear Dynamics*, vol. 73, no. 1-2, pp. 1035–1043, 2013.

[43] H.-X. Ge, F. Lv, P.-J. Zheng, and R.-J. Cheng, "The time-dependent Ginzburg-Landau equation for car-following model considering anticipation-driving behavior," *Nonlinear Dynamics*, vol. 76, no. 2, pp. 1497–1501, 2014.

[44] W.-X. Zhu and H. M. Zhang, "Analysis of mixed traffic flow with human-driving and autonomous cars based on car-following model," *Physica A: Statistical Mechanics and Its Applications*, vol. 496, pp. 274–285, 2018.

[45] J. Monteil, J. Billot, N. E. Sau, and F. El, "Linear and weakly nonlinear stability analyses of cooperative car-following models," *IEEE Transactions on Intelligent Transportation Systems*, vol. 15, pp. 2001–2013, 2014.

[46] Y.-M. Yuan, R. Jiang, M.-B. Hu, Q.-S. Wu, and R. Wang, "Traffic flow characteristics in a mixed traffic system consisting of ACC vehicles and manual vehicles: a hybrid modelling approach," *Physica A: Statistical Mechanics and Its Applications*, vol. 388, no. 12, pp. 2483–2491, 2009.

[47] Z. Yao, R. Hu, Y. Wang, Y. Jiang, B. Ran, and Y. Chen, "Stability analysis and the fundamental diagram for mixed

connected automated and human-driven vehicles," *Physica A: Statistical Mechanics and Its Applications*, vol. 533, p. 121931, 2019.

[48] M. Bando, K. Hasebe, A. Nakayama, A. Shibata, and Y. Sugiyama, "Dynamical model of traffic congestion and numerical simulation," *Physical Review E*, vol. 51, no. 2, pp. 1035–1042, 1995.

[49] H. Wang, W. Wang, J. Chen, M. Jing, and S. Wang, "Estimating equilibrium speed-spacing relationship from dynamic trajectory data," in *Proceedings of the Transportation Research Board 91st Annual Meeting*, Washington, DC, USA, January 2012.

[50] D. Ngoduy, "Platoon-based macroscopic model for intelligent traffic flow," *Transportmetrica B: Transport Dynamics*, vol. 1, no. 2, pp. 153–169, 2013.

[51] H. X. Ge, S. Q. Dai, L. Y. Dong, and Y. Xue, "Stabilization effect of traffic flow in an extended car-following model based on an intelligent transportation system application," *Physical Review E*, vol. 70, no. 6, p. 066134, 2004.

[52] T. S. Chow, "Operational analysis of a traffic dynamics problem," *Operations Research*, vol. 6, pp. 165–184, 1958.

[53] R. Liu and X. Li, "Stability analysis of a multi-phase car-following model," *Physica A: Statistical Mechanics and Its Applications*, vol. 392, no. 11, pp. 2660–2671, 2013.

[54] J. Wang, R. Liu, and F. O. Montgomery, "A car following model for motorway traffic," *Transportation Research Record: Journal of the Transportation Research Board*, vol. 1934, pp. 33–42, 2005.

[55] R. E. Wilson and J. A. Ward, "Car-following models: fifty years of linear stability analysis-a mathematical perspective," *Transportation Planning and Technology*, vol. 34, no. 1, pp. 3–18, 2011.

[56] J. M. D. Castillo and F. G. Benítez, "On the functional form of the speed-density relationship-I: general theory," *Transportation Research Part B: Methodological*, vol. 29, no. 5, pp. 373–389, 1995.

[57] M. Treiber and A. Kesting, *Traffic Flow Dynamics*, Springer, Berlin, Germany, 2013.

[58] K. Ahn, H. Rakha, A. Trani, and M. Van Aerde, "Estimating vehicle fuel consumption and emissions based on instantaneous speed and acceleration levels," *Journal of Transportation Engineering*, vol. 128, no. 2, pp. 182–190, 2002.

[59] T. Tang, J. Li, Y. Wang, and G. Yu, "Vehicle's fuel consumption of car-following models," *Science China Technological Sciences*, vol. 56, no. 5, pp. 1307–1312, 2013.

[60] X. Zhao and Z. Gao, "A new car-following model: full velocity and acceleration difference model," *The European Physical Journal B-Condensed Matter and Complex Systems*, vol. 47, pp. 145–215, 2005.

[61] H. Rakha, M. Van Aerde, K. Ahn, and A. Trani, "Requirements for evaluating traffic signal control impacts on energy and emissions based on instantaneous speed and acceleration measurements," *Transportation Research Record: Journal of the Transportation Research Board*, vol. 1738, no. 1, pp. 56–67, 2000.

[62] W. Shi and Y. Xue, "Study on stability and energy consumption in typical car-following models," *Journal of Physics A*, vol. 381, pp. 399–406, 2007.

[63] T. Q. Tang, J. G. Li, H. J. Huang, and X. B. Yang, "A car-following model with real-time road conditions and numerical tests," *Measurement*, vol. 48, pp. 63–76, 2014.

[64] C. Wu, G. Zhao, and B. Ou, "A fuel economy optimization system with applications in vehicles with human drivers and autonomous vehicles," *Transportation Research Part D: Transport and Environment*, vol. 16, no. 7, pp. 515–524, 2011.

[65] K. Ahn, *Microscopic Fuel Consumption and Emission Modeling, Civil and Environmental Engineering*, Virginia Polytechnic Institute and State University, Blacksburg, VA, USA, 1998.